

**WAVES IN ELECTRON BEAMS HAVING SPACE
CHARGE DEPRESSION OF POTENTIAL**

by

Walter R. Bean

Thesis submitted to the Faculty of the Graduate School
of the University of Maryland in partial
fulfillment of the requirements for the
degree of Doctor of Philosophy

1953

UMI Number: DP70069

All rights reserved

INFORMATION TO ALL USERS

The quality of this reproduction is dependent upon the quality of the copy submitted.

In the unlikely event that the author did not send a complete manuscript and there are missing pages, these will be noted. Also, if material had to be removed, a note will indicate the deletion.



UMI DP70069

Published by ProQuest LLC (2015). Copyright in the Dissertation held by the Author.

Microform Edition © ProQuest LLC.

All rights reserved. This work is protected against unauthorized copying under Title 17, United States Code



ProQuest LLC.
789 East Eisenhower Parkway
P.O. Box 1346
Ann Arbor, MI 48106 - 1346

TABLE OF CONTENTS

	Page No.
LIST OF SYMBOLS	iv
LIST OF FIGURES AND PLATES	vi
CHAPTER I - INTRODUCTION	1
CHAPTER II - THEORETICAL CONSIDERATION	2
The differential equation	3
Thin coupled beams at a distance	4
Cartesian case, continuous velocity distribution	9
Computed solutions for cylindrical beams	14
CHAPTER III - EXPERIMENTAL INVESTIGATION	18
Equipment	18
Experiments performed	19
SELECTED BIBLIOGRAPHY	24
APPENDIX 1 - DERIVATION OF THE WAVE EQUATION, SIMPLE SOLUTIONS.	25
APPENDIX 2 - MIXED BEAMS	30
APPENDIX 3 - VELOCITY DISTRIBUTIONS	33
APPENDIX 4 - ANALYSIS OF HAEFF'S DATA	36
APPENDIX 5 - WAVES IN TWO LINEARLY COUPLED SYSTEMS WITH DIFFERENT PHASE VELOCITIES	39
FIGURES AND PLATES	41
ACKNOWLEDGEMENTS	62

LIST OF SYMBOLS

- a distance between thin beams
 \vec{B} magnetic flux density vector
 $c = \frac{1}{\sqrt{\mu_0 \epsilon_0}}$ the velocity of light in free space
 \vec{E} the electric field vector
 \vec{E}_t the component of \vec{E} normal to the z axis
 E_r, E_θ, E_z cylindrical components of \vec{E}
 E_x, E_y, E_z Cartesian components of \vec{E}
 E'_z, E''_z the first and second derivatives of E_z with respect to r or x
 e the electronic charge = 1.6×10^{-19} coulombs
 $f'(v_0)$ the derivative of the density function of ω_0^2
 \vec{H} the magnetic field vector
 I beam current
 $j = \sqrt{-1}$
 k a coupling coefficient, dimensionless
 m the electronic mass = 9.1×10^{-31} kg.
 p the plasma frequency reduction factor
 Q_n the integral of ω_0^2 with respect to x in a beam
 r, θ, z cylindrical coordinates
 $R_n = \frac{Q_n}{\omega v_0}$ dimensionless beam parameter
 t time
 $u = \frac{\omega + j\gamma v_0(x)}{v'_0}$ a derived variable
 u_A, u_B values of u at $x = x_A, x_B$
 V_{A_1}, V_{A_2} , etc. anode voltage with respect to cathode
 V_{coll} collector voltage with respect to cathode
 $V_{Dr. tube}$ drift tube voltage with respect to cathode
 ΔV difference in voltages in a double stream
 \vec{v} the electron velocity vector, expressing velocity as a function of x, y, z, t or r, θ, z, t .
 v_r, v_θ, v_z cylindrical components of \vec{v}

- v_x, v_y, v_z Cartesian components of \bar{v}
 v_o time average of v_z
 v_o' derivative of v_o with respect to x
 $v_{o.o}$ velocity at center of beam
 $v_o(r), v_o(x)$ v_o as function of position
 V_o potential at center of beam
 v_1 AC part of v_z
 v_n value of v_o for the n^{th} beam
 x, y, z Cartesian coordinates
 x_A, x_B values of x at the beam edges
 γ propagation constant of waves
 δ fractional separation of beam velocities
 ϵ_o permittivity of free space = $\frac{1}{36\pi \times 10^9}$ (MKS)
 θ_1, θ_2 phase constants for waves 1 and 2
 $\lambda = e \frac{\omega a}{v_o}$ dimensionless spacing parameter
 λ_e electron wavelength, distance electron travels in one cycle of the operating frequency
 λ_p plasma wavelength = $\frac{\omega}{\omega_o} \lambda_e$, or more generally $\frac{\omega}{p\omega_o} \lambda_e$.
 μ_o permeability of free space = $4\pi \times 10^{-7}$ (MKS)
 ρ space charge density as function of x, y, z, t or r, θ, z, t
 ρ_o time average of ρ
 ρ_1 AC part of ρ
 τ transit time through R.F. gap in resonant cavity
 ω operating angular frequency
 $\omega_o = \sqrt{\frac{\rho_o e}{m\epsilon_o}}$ plasma angular frequency
 $\omega_{o.n}$ value of ω_o for the n^{th} beam
 ∇ the vector operator
 A^* complex conjugate of A
 ∇_t^2 the Laplacian operator applying to the transverse component of \bar{E}
 $\epsilon = 1 + \frac{j\gamma v_o}{\omega}$ dimensionless quantity related to propagation constant

LIST OF FIGURES AND PLATES

- Figure 1 Cross section of model for analysis of three thin beams side by side.
- Figure 2 Loci of propagation constant versus current in center beam.
- Figure 3 Loci of propagation constant versus beam spacing parameter.
- Figure 4 Loci of propagation constant versus fractional velocity separation.
- Figure 5 Loci of zeros of solutions of Equation (11).
- Figure 6 Loci of zeros of solutions of Equation (12).
- Figure 7 Geometric relations which must be satisfied at end points of solutions, Cartesian beam solution.
- Figure 8 Computed velocities of fundamental and higher order modes of slipping and univelocity beams, cylindrical beam solution.
- Figure 9 Diagram showing basic features of variable length two-cavity demountable tube.
- Figure 10 Block diagram of system used in experimental work.
- Figure 11 Output voltage vs. drift tube voltage, for pulsed and continuous single beam.
- Figure 12 Observed output versus drift voltage for different drift lengths in two cavity demountable tube.
- Figure 13 Electron plasma frequency from plasma wavelength measurements.
- Figure 14 Basic parts of tube of the type used by Haeff.
- Figure 15 Observed output voltages illustrating gain at low collector voltage.
- Figure 16 Experimental data showing similarity of output of tube with low collector voltage to that of a simple double stream amplifier. Theoretically, curves should be parabolic.
- Figure 17 Curves illustrating conditions for gain in a mixed beam.
- Figure 18 Contour maps showing the effect of adding a third stream to a double stream amplifier.
- Figure 19 Hypothetical electron paths which would produce a double stream effect in a gridded gun.
- Plate 1 Photograph of complete apparatus.
- Plate 2 Closeup of demountable tube, illustrating construction and basic parts.

CHAPTER I

INTRODUCTION

This study was initiated because of interest in the work reported by A. V. Haeff (2), in which amplification was discovered in a single beam of moving electrons. In the same paper, results of experiments on a mixed pair of electron beams of different velocities were reported, and a simple theory of amplification in such a mixed beam was presented. The single beam amplification was explained on the basis of the space charge depression of potential in the beam (see Appendix 3). Experimental data indicated gains of 60 db were possible in this device, in fact the gains were as good as those of the double beam tubes tested:

The theory which was used to explain the double stream gain, as is shown later, gives results which indicate that no gain may be obtained in an electron stream unless two groups of electrons of finitely different velocities dominate the situation. The existence of gain due to depression of potential, where a more or less continuous velocity range of electrons exists, is controversial. The basic difference in the two cases is that the space charge depressed beam has a spatial distribution of electrons, in contrast to the assumed homogeneous mixture of the theory.

Shortly after the publication of this paper, the writer visited Dr. Haeff. At that time Dr. Haeff expressed interest in determining the actual electron velocities in the single stream tube, but this was never done. Some time later it was decided by the author to attack theoretically the problem of wave propagation in the space charge depressed beam, and to attempt to repeat Haeff's experiment, with conditions more closely related to those which can be treated theoretically.

CHAPTER II

THEORETICAL CONSIDERATIONS

The basic methods used in solving problems of wave propagation in electron streams were established by Hahn (3) and Ramo (12). This procedure, originally applied to the klystron, involves certain limiting assumptions:

1. All time-varying quantities in the beam are assumed to be much smaller than the corresponding static values, except for the electric and magnetic fields, which may not exist except in the presence of disturbances.

2. Wave functions are assumed to be harmonic and of the form $f(x,y)e^{j\omega t - \gamma z}$. ω is the angular frequency of the disturbance, t is time, z the distance in the direction of wave propagation, and γ is the propagation constant, which indicates the velocity of propagation and/or rate of amplification or attenuation.

Other assumptions may be necessary for a particular problem. The general Hahn-Ramo method solves the problem by proceeding directly from Maxwell's equations and the equations of continuity of charge and of motion of a charged body. A characteristic equation is usually found, the solutions of which give characteristic values of γ . In some cases, in particular those of continuous velocity distributions, no characteristic equation exists, for the solutions are dependent on the impressed boundary conditions of a differential equation. This differential equation is derived in Appendix 1, and is discussed subsequently.

Macfarlane and Hay have published a theoretical paper entitled "The Slipping Stream Amplifier" (6). They obtain results in which amplification is obtained in a beam in which there is a velocity gradient in a direction transverse to the motion of the electrons. A close examina-

tion reveals that the solution is quite dependent on the presence of a transverse magnetic field and transverse electron motion. The tube described operates in many ways like a magnetron. In such a tube the crossed electric and magnetic fields allow the electrons to move into positions in which they may interact with fields of the proper phase to cause energy to be given up to the fields by the electrons. The type of tube described by Haeff could not possibly have operated in such a mode, since no transverse DC electric and magnetic fields were present.

Several writers (9) (11) have published theoretical papers on the amplification characteristics of two thin laminar electron beams in cylindrical coordinates. These results illustrate the decrease in gain produced when the two groups of electrons are physically separated. They do not, however, shed light on the continuous type of velocity distribution

Birdsall (1) and Haus (4) have attacked the problem of a homogeneous electron beam with arbitrary velocity distribution, extended to finite beams. They reach the general conclusion that in order for a beam to have gain modes, the electrons must have a velocity distribution having two peaks, separated by a region of velocity in which there are relatively few electrons. It is interesting to note that in neither case did the author succeed in obtaining an analytical criterion for gain. This is, unfortunately, the usual result.

The Differential Equation. The equation which must be solved in the analysis of a "slipping" stream, derived in Appendix 1, is written below for a two-dimensional Cartesian beam and a θ independent cylindrical beam.

$$\frac{d^2 E_z}{dx^2} + \left(\gamma^2 + \frac{\omega^2}{c^2}\right) \left(1 + \frac{\omega_o^2}{[j\omega - \gamma v_o(x)]^2}\right) E_z = 0 \quad (1)$$

$$\frac{d^2 E_z}{dr^2} + \frac{1}{r} \frac{dE_z}{dr} + \left(\gamma^2 + \frac{\omega^2}{c^2}\right) \left(1 + \frac{\omega_o^2}{[j\omega - \gamma v_o(r)]^2}\right) E_z = 0 \quad (2)$$

The special choice of velocity functions $v_o(x)$ and $v_o(r)$ is taken up in Appendix 3. The choice of boundary conditions is not limited. Those

conditions which seem most natural are ones in which the beam is located in free space or is surrounded by perfectly conducting metal walls. The problems are much simplified if these walls are just at the edge of the beam itself. Other, more complicated boundary walls may be imagined, but do not bear on the present problem.

If a cylindrical beam is considered, one boundary condition is $E_z^i = \frac{dE_z}{dr} = 0$ at $r = 0$. This is necessitated by the physical requirement that the fields be finite everywhere for the cylindrical equation (2) has two independent solutions, one of which is finite at the origin, the other infinite. The finite solution has a zero derivative at the origin. A second boundary condition is that E_z is zero at the conducting wall outside the beam. If the beam is in free space, the solution must approach zero at infinity. A Cartesian beam has $E_z = 0$ at conducting walls; if it is in free space, the solution at infinity must vanish.

If two boundary conditions be placed on solutions of (1) or (2), as is the case, only certain values of γ will satisfy both. These are to be determined. A priori it might seem logical to attempt to apply the W.B.K. (Wentzel, Brillouin, Kramers) method (5) to this problem, but the limitations of this method prohibit its use. Our approach will be first by means of analysis of laminar beams with discrete velocities and then by an almost exact solution of the Cartesian case.

Thin coupled beams at a distance. Our first approach to the problem of a space charge depressed electron beam is the analysis of electron beams which are decoupled from one another by moving them apart. Common sense predicts that two beams which give a certain amount of gain when well mixed, will give less as they are moved apart so that their coupling fields interact less. An interesting problem is that of adding a third beam of intermediate position and velocity to a set of two beams.

This will be treated using as the model a thin beam (thin in the x direction) which extends to infinity in the y direction and travels parallel to the z axis in which direction it is very long. Because the

beam is taken infinitesimally thin (for mathematical convenience), it does not suffice to make the space charge density finite. It must be infinite, in such a way that $\int_{\text{Beam}} \rho_{\text{Across}} dx = \text{const.}$ The beam may then be considered the limit of a physical beam as the width is decreased to zero.

The equation to be solved now is (1). Consider three beams side by side, as in Fig. 1. The spacing is a , and space charge in the two outer beams is the same, while that in the center beam may be varied independently. The three beams have velocities $v_0(1-\delta)$, v_0 , and $v_0(1+\delta)$. δ is a measure of the fractional velocity difference of the beams. They are in free space.

Values of γ sought are always near $j\omega/v_0$, for reasons made apparent in Appendix I. It is convenient to use this as an approximation to γ for the solution outside the beams; in this region, the equation becomes

$$E_z'' + (\gamma^2 + \frac{\omega^2}{c^2})E_z = 0 \quad (3)$$

A further approximation concerns the relative values of v and c , the velocity of light. We assume $v \ll c$, and leave out the ω/c term, obtaining $E_z'' + \gamma^2 E_z = 0$, or approximately (3a) $E_z'' - \frac{\omega^2}{v_0^2} E_z = 0$. This equation has the elementary solutions $e^{\pm \frac{\omega}{v_0} x}$. The only difference, physically, between this solution and the exact one, is a small change in the way in which the fields decay away from the beams. There are four regions in which the solutions of (3a) are found. They shall be denoted as follows:

$$\begin{aligned} x < -a & \quad E_z = A_1 e^{\frac{\omega x}{v_0}} \\ -a < x < 0 & \quad E_z = A_2 e^{\frac{\omega x}{v_0}} + B_2 e^{-\frac{\omega x}{v_0}} \\ 0 < x < a & \quad E_z = A_3 e^{\frac{\omega x}{v_0}} + B_3 e^{-\frac{\omega x}{v_0}} \\ a < x & \quad E_z = B_4 e^{-\frac{\omega x}{v_0}} \end{aligned}$$

The conditions under which the A_n and B_n may be eliminated are the requirements of continuity of the solutions of E_z and of its first derivative. The use of infinitesimally thin beams results in a slightly different condition, for if equation (1) be integrated across one of the

beams (from $x - \epsilon$ to $x + \epsilon$), the equation becomes

$$E'_z(x+\epsilon) - E'_z(x-\epsilon) + E_z \left(\gamma^2 + \frac{\omega^2}{c^2} \right) \int_{x-\epsilon}^{x+\epsilon} \frac{\omega_{on}^2}{(j\omega - \gamma v_n)^2} dx = 0. \quad (4)$$

v_n represents the velocity of the particular beam, ω_{on} the plasma frequency. If Q_n be made to denote $\int_{x-\epsilon}^{x+\epsilon} \omega_{on}^2 dx$ and letting $(\gamma^2 + \frac{\omega^2}{c^2})$ be approximated by $-\frac{\omega^2}{v_o^2}$, (4) becomes

$$E'_z(x+\epsilon) - E'_z(x-\epsilon) \simeq \frac{\omega^2}{v_o^2} \frac{Q_n E_z}{(j\omega - \gamma v_n)^2} \quad (4a)$$

The relations which the four solutions and their derivatives with respect to x must satisfy are collected below.

$$\begin{aligned} \text{at } x = -a: \quad & A_1 e^{\frac{-\omega a}{v_o}} = A_2 e^{\frac{-\omega a}{v_o}} + B_2 e^{\frac{\omega a}{v_o}} \\ & A_1 e^{\frac{-\omega a}{v_o}} \left(\frac{\omega}{v_o P_1} \right) = \frac{\omega}{v_o} [A_2 e^{\frac{-\omega a}{v_o}} - B_2 e^{\frac{\omega a}{v_o}} - A_1 e^{\frac{-\omega a}{v_o}}] \end{aligned} \quad (5)$$

$$\begin{aligned} \text{at } x = 0: \quad & A_2 + B_2 = A_3 + B_3 \\ & (A_2 + B_2) \left(\frac{\omega}{v_o P_2} \right) = \frac{\omega}{v_o} [A_3 - B_3 - A_2 + B_2] \end{aligned}$$

$$\begin{aligned} \text{at } x = +a: \quad & A_3 e^{\frac{\omega a}{v_o}} + B_3 e^{\frac{-\omega a}{v_o}} = B_4 e^{\frac{-\omega a}{v_o}} \\ & B_4 e^{\frac{-\omega a}{v_o}} \left(\frac{\omega}{v_o P_3} \right) = \frac{\omega}{v_o} [-B_4 e^{\frac{-\omega a}{v_o}} - A_3 e^{\frac{\omega a}{v_o}} + B_3 e^{\frac{-\omega a}{v_o}}] \end{aligned}$$

The P_n quantities represent $\frac{v_o(j\omega - \gamma v_n)^2}{\omega Q_n}$. In order that these six equations be consistent, the determinant of the coefficients of A_n and B_n must be zero. Let us define a dimensionless beam spacing parameter $\lambda = e^{\frac{\omega a}{v_o}}$. The determinantal equation after quite a bit of reduction is found to be

$$\begin{aligned} & 8\lambda^4 P_1 P_2 P_3 + 4\lambda^4 (P_1 P_2 + P_2 P_3 + P_1 P_3) \\ & + 2(\lambda^4 - 1)P_2 + 2\lambda^2(\lambda^2 - 1)(P_1 P_3) + (1 - \lambda^2)^2 = 0 \end{aligned} \quad (6)$$

This relation is of the sixth degree in γ , but if $Q_1 = Q_3$ (space charge in outer beams equal), it reduces to a cubic. Since the relation would have entirely real coefficients for a variable $j\gamma$, the solutions must be satisfied for both $j\gamma$ and $(j\gamma)^*$, which means that if one solution

has a real part α , another has the same imaginary part but real part $-\alpha$.

A new variable is now defined, which measures the difference of γ from a non-growing wave with phase velocity v_0 . Thus we let $\gamma = \frac{j\omega}{v_0} (1-\epsilon)$, and $\epsilon = 1 - \frac{\gamma}{\frac{j\omega}{v_0}}$. It is necessary in reducing (6) to make the approximation $\gamma\delta v_0 = j\omega\delta$, but the quantity appears in a position of secondary importance. Final reduction of (6) gives

$$\begin{aligned} \epsilon^6 + \epsilon^4(-2\delta^2 - R_1 - \frac{R_2}{2}) + \epsilon^2[\delta^4 - R_1\delta^2 + R_2\delta^2 \\ + \frac{R_1R_2}{2}(1 - \frac{1}{\lambda^2}) + \frac{R_1^2}{4}(1 - \frac{1}{\lambda^4})] \\ + [-\frac{\delta^4R_2}{2} + R_1R_2\frac{\delta^2}{2}(1 - \frac{1}{\lambda^2}) - \frac{R_1^2R_2}{8}(1 - \frac{1}{\lambda^2})^2] = 0 \end{aligned} \quad (7)$$

The new quantity R is given by $R_n = \frac{\omega}{v_0} \frac{\int \omega_0^2 dx}{\omega^2} = \frac{Q_n}{\omega v_0}$, where the integral is taken from one side to the other of the n^{th} beam.

Figures 2, 3, 4 show the effect of varying each of the parameters R , δ , λ , by plotting the loci which the six characteristic values of ϵ take as one parameter at a time is changed.

In each case R , λ , or δ is varied, and the locus of the values ϵ plotted as the parameter is varied. In all cases there are six modes. They appear in two sets of three which are negatives. This is because of the equation's being a function of ϵ^2 . Two of each of these three are complex conjugates for certain ranges of the parameters, indicating modes with gain and attenuation. Two of the six modes are always purely propagational, and have large real ϵ .

In the Figures, liberty has been taken to multiply δ^2 , R and ϵ^2 by a factor which makes their magnitudes of the order of unity. Practical values of δ^2 would be .01 or less and would result in values of ϵ of the order of .1 with R in the neighborhood of .01. The physical significance of λ , ϵ , and δ has been explained; $R = \frac{\omega}{v_0} \frac{Q}{\omega^2}$, and can be calculated for

a finite beam of width W : $R = \frac{\omega}{v_0} \cdot \frac{\omega_0^2 W}{\omega^2} = \frac{2\pi W}{\lambda_e} \cdot \frac{\omega_0^2}{\omega^2}$. λ_e is the distance traveled by an electron at velocity v_0 during one cycle of the operating frequency. For beams narrow compared to λ_e , $\frac{2\pi W}{\lambda_e}$ may be of the order of 1, $\frac{\omega_0^2}{\omega^2}$ is commonly .01 or less, making R of the order of .01.

The curve of Figure 2 shows the decrease of gain occasioned by addition of current to the center beam. Gain vanishes completely when the current in the center beam equals 65% of that in each of the others. Oddly, the current in the center beam affects very little the two propagational modes.

Figure 3 indicates the effects of increasing beam spacing. The gain decreases while the phase velocity of the modes remains constant until, for $\lambda = 1.31$, gain disappears. Again, the two purely propagational modes, being functions of the two outer beams, vary but little.

The final curve, Figure 4, shows what happens as δ , the velocity separation, is varied. For small velocity difference, interaction is insufficient to produce gain, as is also true for excessively high velocity difference.

For the special case of zero current in the center beam, it is simple to invoke a limiting condition for gain (the zero discriminant of the resulting quadratic). This gives as a criterion for the presence of gain

$$\delta^4 - R_1 \delta^2 + \frac{R_1^2}{4} \left(1 - \frac{1}{\lambda^4}\right) < 0 . \quad (8)$$

When the third beam is present, it is still possible to set up a condition of this type, but it is much less simple.

The same method may be employed to solve the problem of four or more thin beams in free space, but it is easy to imagine the greater difficulty as the number of equations increases. When the method is applied to a thin cylindrical beam, as is formulated by Parzen (9), the coefficients in each equation are not simply $e^{\frac{\omega a}{v_0}}$, but zero and first order Bessel functions. Criteria for gain are correspondingly difficult to

obtain and there is nothing to indicate that the results would be vitally different from those of the Cartesian problem.

The point to be made by the foregoing is that the physical separation of beams with discrete velocity differences does not introduce any new effects but merely decreases tendency toward amplification. The addition of conducting walls near the beam will have some effect on the gain, in general to decrease it, since the E_z will be less everywhere, going to zero at the conductor instead of at infinity. Less longitudinal field will produce less beam interaction, and give less gain.

Cartesian case, continuous velocity distribution. Equation (1) may be solved almost exactly, for arbitrary boundary conditions, by use of a transformation of variables¹. The equation must be simplified by elimination of the velocity of light term $\frac{\omega^2}{c^2}$. The equation which can be solved is

$$\frac{d^2 E_z}{dx^2} + \gamma^2 \left(1 + \frac{\omega_o^2}{[j\omega - \gamma v_o(x)]^2} \right) E_z = 0 \quad (9)$$

The velocity $v_o(x)$ is assumed linear in x , which is sufficiently general to be of interest. The substitution $u = \frac{\omega + j\gamma v_o(x)}{\frac{dv_o}{dx}}$ is made, and if $\frac{dv_o}{dx}$

be denoted by v'_o , the equation (9) reduces to the form

$$\frac{d^2 E_z}{du^2} - \left(1 - \frac{\omega_o^2}{v_o'^2 u^2} \right) E_z = 0, \quad (10)$$

which is free of explicit dependence on γ . The boundary conditions are considerably altered. If the beam is enclosed at each edge by conducting planes, the conditions there are still $E_z = 0$; if the beam is in free space, the solution of $E_z'' + \gamma^2 E_z = 0$, outside the beam must be $e^{j\gamma x}$ on the positive x side, so $\frac{1}{E_z} \frac{dE_z}{dx} = +j\gamma$ is replaced by $\frac{1}{E_z} \frac{dE_z}{du} = -1$. On the negative x side, the condition is the negative of this.

The unknown quantity is the mapping of the range of x across the beam into the complex u plane. Herein lies the most important step. Certainly, (10) contains no reference to beam width, and conducting plates

¹First used by Macfarlane and Hay (6), on a different problem.

in the physical model certainly have no similar representation in the u plane. As it happens, the problem must be solved in a backhanded (perhaps even underhanded) way. Two values of u (u_A and u_B) must be found at which the boundary conditions at the beam edges (x_A and x_B) are satisfied. It will be shown that there are infinitely many sets of such values of u . u_A and u_B also must satisfy other conditions, in that for some complex γ and for given $v(x_A)$ and $v(x_B)$ they must transform into real values of x . For given $v(x_A)$ and $v(x_B)$ there are a countable set of such u_A and u_B .

Figure 7 shows two points, marked A and B, in the complex u plane. In Appendix 3 it is shown that for linear velocity variation, $v'_0 = \omega_0$. This is the case that will be discussed. The additional requirements on u_A and u_B are illustrated. Since u is linear in x and, more directly, in $v_0(x)$, note that the line joining u_A and u_B must pass through $u = \frac{\omega}{dv_0/dx} = \frac{\omega}{v'_0} = \frac{\omega}{\omega_0}$. (For practical tubes $\frac{\omega}{\omega_0}$ is of the order of 10 or greater.) u_A and u_B must also be the proper distances from $u = \frac{\omega}{\omega_0}$ so that the ratio of these distances equals the ratio of v_A to v_B . A further requirement may be placed upon gain modes, namely that u_A and u_B fall in the first and second quadrants of the u plane, or, alternately, in the fourth and third quadrants. This is necessary for reasons given in Appendix 5. The meaning of such a requirement, physically, is that the phase velocity of the growing wave cannot be greater than the velocity of the fastest electrons or less than that of the slowest.

Now that it has been established how the values u_A , u_B must lie, we shall investigate what properties $E_z(u)$, the solution to (10) must have at these points. The simplest boundary conditions; those of conducting walls at x_A and x_B , require $E_z(x_A) = E_z(x_B) = 0 = E_z(u_A) = E_z(u_B)$. The solution $E_z(u)$ must, then, have zeros at u_A and u_B , in which case, if the u_A and u_B satisfy the other stated conditions, $E_z(u)$ along the line joining u_A and u_B gives the solution along the corresponding segment of the x -axis. No other part of the u plane affects this particular solution.

In order to find u_A and u_B satisfying the requirements, $E_z(u)$ must be determined over a large part of the complex u plane. Even more than this, since (10) is of the second order, $E_z(u)$ may be any of a wide range of functions. This wide range of functions are all linear combinations of two independent solutions of (10). Let a particular pair be called $f_1(u)$ and $f_2(u)$. The general solution is $f_1(u) - \phi f_2(u)$, in which ϕ is an arbitrary complex number. All we are really interested in about the solutions is their zeros, since u_A and u_B must be picked from them. A zero of $f_1 - \phi f_2$ makes $\phi = \frac{f_1}{f_2}$. All zeros of all linear combinations can be found by plotting $\frac{f_1}{f_2}$. If we choose a point in the u plane at random, and $\phi = \phi_0$ there, we search for other points where $\frac{f_1}{f_2} = \phi_0$. These points are all zeros of some particular solution of (10). Usually, curves can be drawn in the u plane along which $\frac{f_1}{f_2}$ varies periodically through the same set of values. These we shall call the loci of zeros of the solutions, and on these the next arguments will be based.

Let us consider the equation

$$\frac{d^2 E_z}{du^2} + \frac{1}{u^2} E_z = 0. \quad (11)$$

For u sufficiently less than unity in absolute value, (10) reduces to (11). Similarly, the solutions of (10) will become asymptotic to those of (11) in the same region.

The solutions of (11) are relatively simple. Two of them are $\sqrt{u} \sin\left(\frac{\sqrt{3}}{2} \ln u\right)$ and $\sqrt{u} \cos\left(\frac{\sqrt{3}}{2} \ln u\right)$. The zeros of these functions lie on the positive real u axis, since values of u on the positive real axis map onto both sides of the real $\ln u$ axis, on which all the zeros of $\sin Z$ and $\cos Z$ are located. The zeros of these two functions are shown plotted vs. $\ln u$ in Figure 5. They are equally spaced in the $\ln u$ plane, but crowd together at $u = 0$ in the u plane. The function which is the ratio of these, $\tan\left(\frac{\sqrt{3}}{2} \ln u\right)$, has its zeros where the zeros of $\sin\left(\frac{\sqrt{3}}{2} \ln u\right)$ are, and poles where the zeros of $\cos\left(\frac{\sqrt{3}}{2} \ln u\right)$ are. The loci of zeros of arbitrary solutions of (11) in the $\ln u$ plane are horizontal lines. In the u plane these become radial lines.

The next step is to determine in what way the loci of zeros of solutions of (10) differ from these radial lines.

If ju is substituted for u in (10), the equation becomes

$$\frac{d^2 E_z}{d(ju)^2} + \left(1 + \frac{1}{(ju)^2}\right) E_z = 0. \quad (12)$$

For real ju , that is, imaginary u , the solutions of (12) will be oscillatory, with zeros lying on the $\text{Im } u$ axis as shown on the left side of Figure 6. The accumulation of zeros toward the origin indicates a branch point and essential singularity there as in the asymptotic functions. The loci of zeros of arbitrary solutions of (12), which also qualify as zeros of solutions of (10), lie as illustrated in the other part of Figure 6. Since $f(-u)$ and $f(u)$ are both functions satisfying (10), all loci have negative counterparts.

The search for points which satisfy all requirements on u_A and u_B is fruitless, for none of the loci illustrated in Figure 6 could pass through two such points as are shown in Figure 7. We conclude that no gain modes are possible.

This having been established, we turn to the modes which do not give gain. Their u_A and u_B are not limited by requirements of falling into certain quadrants, as they lie on the real u axis. They must, however, be spaced appropriately with respect to the $\frac{\omega}{\omega_0}$ point. Within the limitations of u_A and u_B for a particular set of v_A and v_B , two sets of appropriate points u_A and u_B can be found, one set of which lies on the positive real axis, one on the negative real axis. These give rise to two sets of characteristic values of γ , one of which gives waves with phase velocity $>v_A$ and the other with phase velocity $<v_B$, so no possible waves have the velocity of any of the electrons. The lowest modes, with velocity most different from electron velocities, have E_z of uniform sign from x_A to x_B ; the next modes, with velocities closer to electron velocities, have E_z positive for some part of the beam, negative for the rest. Such a mode is hard to detect, for most detectors indicate an integrated value of the field over the beam. The other modes are of successively

higher order, and their only importance in practice is the power which they make unavailable for output. The modes of the Cartesian coordinate beam have velocities very similar to those calculated for a cylindrical beam in Figure 8.

It is possible to find modes with very large gain when $\omega_0 \cong \omega$. These may be interpreted as oscillations of the plasma. They are not practical for use in a tube, for in addition to the inherent instability, the problem of attaining plasma frequencies of the order of 3000 mc. is difficult. An additional complication is the large difference in velocity across the beam required to satisfy these modes.

We return to the solutions of equation (10) when the velocity gradient v'_0 is greater than or less than ω_0 . The form of the solutions will be similar to those discussed above for smaller velocity gradients, except the characteristic values of the propagation constant γ will be more tightly grouped. If the gradient v'_0 equals or exceeds $2\omega_0$, the mathematical solutions show only two possible values of γ , which give velocities corresponding to the beam velocity at the two edges. For velocity gradients of this size, the assumption of a plane wave solution is somewhat questionable, anyhow. Particularly simple solutions are derived when $v'_0 = 2\omega_0$, being reducible to Bessel functions. These solutions were examined in detail and found to produce no gain modes.

When the beam is in free space, with no conducting walls, the boundary conditions at the beam edges are $\frac{dE_z}{dx}/E_z = \pm j\gamma v'_0$. In terms of u these are simply $\frac{dE_z}{du}/E_z = \mp 1$. Let us again consider an arbitrary solution of (10), characterized by its locus of zeros. Its derivative function $\frac{dE_z}{du}$ also has zeros along approximately the same line, for the approximate symmetry of the function about the locus requires it. The matching function $\frac{dE_z}{du}/E_z$ has alternating zeros and poles along the locus.

Intuition shows that the points at which the function $\frac{dE_z}{du}/E_z$ has values of ± 1 lie along a line which is very near, but not necessarily coincident with the first. Again, it seems necessary to draw the conclusion that the type of modes which propagate do not include small gain

with small ratio of plasma frequency to operating frequency.

When the beam is enclosed by conducting walls at a distance, the transformation of boundary conditions is complicated. The nature of the free beam solutions for thin laminar beams indicates that moving the conducting walls away from the beam does not introduce new results.

The case of an electron beam in which the velocity distribution has even symmetry about the center is easily investigated, for the symmetry of velocity requires even or odd symmetry in the solution. For odd symmetry, the solution must be zero in the center, which puts it in the class with beams confined by conducting plates. For the solutions with even symmetry, the first derivative must be zero at the center. This gives a boundary condition which may be discussed in the same terms as before. The same conclusion is reached regarding gain.

The changes of importance in the mode pattern are those which occur when the velocity difference or the space charge density is increased. In the former instance, the mode velocities are crowded together, the difference of velocity of the two fundamental modes is increased, and the effect seems the same as an increase in the plasma frequency. When space charge density is increased, the mode velocities are spread farther apart, and again, of course, the plasma frequency is increased.

Changes in plasma wavelength, being determined from the difference in velocity of the two fundamental modes, are probably the only external evidences of slipping of electrons, for plasma wavelength can be measured directly as twice the distance between minima of RF current in the beam. The effect of slipping is probably deleterious to the operation of high current tubes, where bandwidth is already limited by high space charge density, and the increase of effective plasma frequency will cause additional narrowing.

Computed solutions for cylindrical beams. Because of the analytic difficulties in the solution of the general slipping cylindrical beam, it was considered an excellent opportunity when the use of the Institute

for Advanced Study Electronic Digital Computer was made available for work on this problem. It was decided that the writer should prepare the code for the machine, in order that experience in this be available at RCA Laboratories.

The method chosen for preliminary analysis was that of solving (2) for chosen values of γ and attempting to determine whether any γ not purely imaginary could result in solutions which would satisfy the boundary conditions. A complete survey of the γ plane would require excessive time, while a method of iteration and successive approximations might not converge readily when handled by the computer. An attractive method was forward integration of equation (2), satisfying the boundary conditions $E'_z = 0$ at $r = 0$, to the final value of r , at the boundary. The value $E(\gamma, r_{\text{final}})$ might be called $f(\gamma)$. It will be zero for γ satisfying the boundary conditions, and since the coefficients of the equation (2) are regular except at $\gamma = j\omega/v$, the function $f(\gamma)$ will be analytic everywhere in the finite γ plane except on portions of the imaginary axis¹. This leads to the method of counting zeros of a complex function inside a closed contour by counting encirclements of the origin of $f(\gamma)$ as γ traverses a chosen contour, as in a Nyquist plot.

The net number of encirclements of the origin will, in the absence of singularities of the function within the contour, equal the number of zeros in the contour. The application of this to the determination of the presence of gain modes is simple and direct: contours of γ are chosen which do not cross the imaginary axis, and which are of such size and position that all modes of interest would lie inside. γ is traversed point by point, with a sufficiently fine mesh so that any $f(\gamma)$ does not proceed more than 90° between points. Record is made when $f(\gamma)$ crosses the coordinate axes, with due regard to direction. When the contour is closed, four quantities are obtained, being the net number of times each

¹This quality of the solution results from a theorem of Fuchs, see, for example, Copson, Theory of Functions of a Complex Variable, pp. 233-34.

of the four major axes was crossed. These should be all equal to the number of zeros in the contour. This provides a valuable check of the method.

The IAS computer is a 40 digit, parallel, binary high speed general purpose computer, with an internal high speed memory of 1024 words of 40 digits, and at the present time the only external memory is provided by IBM punched cards. Iterative integration procedures, while practical insofar as computation time is concerned, are not desirable because the required memory is too great. The other alternatives to the solution of the differential equation are the forward integration methods. Mainly because of the writer's unfamiliarity with Runge-Kutta and allied methods, a method devised by Milne (7) was employed for integration. This is a simple device, utilizing stored values previously calculated to determine results accurate to fifth differences. It was felt that use of such a method, with the simple means for changing size of increments of r and γ and for handling the complex variables, would be fruitful. The code prepared for the machine solution allowed any values of the constants of the beam to be chosen, with shifting routines to allow increase of the variables outside the limits of the machine, which are ± 1 . A set of checks was included to stop calculation if the increments proved too large for accuracy.

The final code was prepared in two editions. The first of these covered a rectangular contour of γ , making counts of axis crossings as outlined above, and would stop only on completion of the contour. The physical constants such as beam diameter, frequency, etc. could be given any chosen values, and provision was made for considering a beam with conducting boundary at the beam edge, or any finite distance away; this was done by making ω_0 a step function falling to zero at the beam edge. The resulting solution has a discontinuity in the second derivative, which is smoothed out in the function itself. The second edition of the code recorded values of $f(\gamma)$ for γ on a line parallel to the imaginary γ axis, as many as 70 complex values on a single run.

The actual preparation of the code occupied the greater part of a month, and error finding took about three weeks. The statistical chance of error in preparation of punched cards is low, but nonetheless 3 such errors had to be detected by preliminary runs on trigonometric and Bessel functions. Priority of machine time accounted for a delay of several months.

At the time of the initiation of the computing problem, the work on the work on the Cartesian case had not been completed, and the experimental work had not been begun. The results of these indicated that extreme concentration on determination of presence of gain was not necessary. The root-counting code was used only in broad sweeps of the γ plane, and for a practical set of constants this coverage showed that no roots were counted. Smaller segments of the plane were covered, and in no case were any roots discovered. Some indication of the amount of calculation involved is indicated by the amount of time required for a typical contour traverse, 32 minutes. During this time, the machine performed no less than 10^6 elementary operations.

Because of the large amount of time required for the contour traverses, and the small amount of usable data (4 numbers) obtained at the end of each run, it was decided to concentrate on obtaining sets of values of $f(\gamma)$, and this was done. In Figure 8 are shown some mode velocities calculated for a slipping cylindrical stream, as compared with mode velocities of an equivalent univelocity beam. The beam used in this calculation was .080 inches in diameter, inside an .080 inch tube. Beam center voltage was 100 v. and beam current 6 ma. It may be thought desirable to obtain data for all possible physical cases, but the estimated machine operating cost of \$400 per hour and the desperate need of its services by high priority government agencies prevented even consideration of this. The writer is highly indebted to the staff at IAS for the chance to use this excellent machine.

CHAPTER III

EXPERIMENTAL INVESTIGATION

Equipment. In order to attempt to repeat the experiment of Haeff, and also to produce experimental conditions more nearly free of complication, a demountable tube was constructed. This necessitated the building of a vacuum system. The main features of this tube, which is illustrated in plates 1 and 2, are shown graphically in these and in Figure 9. The tube consists of an evacuated brass envelope, enclosed by a glass sleeve. The brass part acts as an aligning jig for the electron gun, the two resonant cavities, the collector, and any other cylindrical electrodes. The electron gun used throughout the investigation has an .050" diameter oxide cathode, and produces a beam which can be readily confined to an .060" diameter through the length of the tube, which is about 15 inches in length from gun to collector. In most of the experiments, the electron beam was confined by a set of molybdenum tapes, which form a drift space .125" on a side. The tapes are only .001" thick, and hence may be made to roll on rollers around the cavities. In this way cavity movement is possible without varying the position of anything else in the tube. The large electromagnet illustrated produces large longitudinal magnetic fields which reduce transverse beam expansion to a very small value. The power supply visible in plate 1 was constructed to enable quick changes to be made in the electrode voltages and to make observation of electrode currents rapid and convenient.

Among the refinements in this demountable tube assembly are: cavities which may be tuned and decoupled from outside the vacuum, tube sides cut away for observation of conditions within the tube, interchangeable collector assembly, and a diaphragm with apertures of graded diameter by which beam size can be approximated by measuring interception of current on the diaphragm. Tuning and adjustment of the beam aperture is

done by means of a rod having a half-gear attached. This can be made to mesh with other gears in the tube to perform these functions. The vacuum system, to which the tube is connected rigidly, can maintain a pressure of 5×10^{-8} mm. Hg absolute at the gage, which for accuracy is mounted in a position of symmetry with respect to the electron gun. The system is completely demountable, being assembled with the use of neoprene O-rings. The high speed of the vacuum pump, 300 liters per second, together with the large size of the liquid nitrogen trap, both contribute toward obtaining the very low pressure in the system.

The radio frequency system is sketched in Figure 10. The signal generator feeds the tube through a tuner. The output is fed through a superheterodyne receiver and observed on either a meter or an oscilloscope tube. The loop in each resonant cavity is fed from the coaxial line through a non-matched hermetic seal. The coaxial line is rigid, and emerges through an O-ring gland seal. Cavities are moved longitudinally by pushing and pulling on this coaxial line; coupling is adjusted by rotating it, which rotates the loop inside the cavity. This has proven to be a satisfactory type of coupling for this type of work, in which little signal power is involved, and large losses are tolerable.

Experiments performed. The initial experiments were designed to determine if increasing waves could be set up in a slipping stream of electrons. In order to insure that positive ion neutralization of the beam would not destroy the velocity difference, experiments with a continuous beam were compared with experiments in which the beam current was pulsed by application of pulsed voltage to a gun electrode. In both these cases the measurement consisted of applying input to the input cavity and observing the output voltage while one of the electrodes was swept in voltage. The voltage of the entire cavity system was swept with respect to the gun electrodes. Typical of the observed wave forms are those shown in Figure 11, for similar conditions, pulsed and continuous. The decrease of output at low voltage is due to decreased cavity coupling caused by long transit times; this factor should be $\left[\frac{\sin r/2}{r/2} \right]^2$, where r is the

transit time through the RF gap of the cavity. In these terms, the observed behavior of the cavities indicated that the effective gap length was .060", as compared with the physical gap length of .040". The maxima and minima of the traces are due to the fundamental wave of the electron stream; velocity modulation of the beam at the input requires that the RF cavity current have such minima. An interesting observation not recorded by any previous experimenter was the non-zero minima of cavity current visible in most of the oscilloscope traces. This must be due to the fact that the finite gap does not excite entirely velocity modulation on the beam, but some current modulation as well. The residual current modulation is of the wrong phase to produce the total cancellation of RF current at the minima. Another reason for this effect is the fact that in a finite beam, the "slow" and "fast" waves do not have the same plasma frequency reduction factor p (See Appendix I). This will give rise to unequal excitation of the two waves.

To overcome the difficulties introduced by the transit time factor, the cavities were moved so as to make the drift space length increase. If exponential gain occurred in the tube, the output vs. drift space voltage curve should not be similar for different tube lengths, but should increase considerably at the low voltage end, where the beam has highest space charge density and greatest slip. In a number of different experiments, using different voltages and currents, no such effect was noticed. Some of the curves are shown in Figure 12. The difference in the pattern of the maxima and minima is due to the difference in the number of electron plasma wave lengths between the cavities, but the envelope of the curves is the same for different tube lengths, indicating no gain.

By observation of the drift tube voltage for each minimum of the output voltage, the plasma frequency can be calculated. This is done in Figure 13. The plasma frequency produced in this exercise is as great as 267.5 megacycles. In some tests, it was 375 mc., and no gain existed. From the known beam diameter and velocity, the amount of the slip can be determined. The amount of gain produced by an equivalent double stream

amplifier with half its electrons having the velocity of the beam center and the other half at the edge velocity would be, for a tube of the length used here, about 30 db. We conclude that it has been illustrated that gain in the electron beams observed due to slipping is non-existent.

There yet remained, following this, to attempt to show the origin of the gain obtained by Dr. Haeff. It was thought, before data on the exact tube constants he used was made available, that the reported phenomena might be due to the velocity change between cavities and drift tube, according to the theory of Tien and Field (13), which postdated Haeff's work. When calculations were applied to these constants, the possibility of explanation on the basis of the velocity jumps was ruled out. The demountable tube was altered to represent the Haeff tube insofar as the drift region is concerned (See Figure 14). The same class of experiments as before was performed, with almost the same results. The only difference was that the drift tube voltage could be operated lower and output still observed, because the relatively high and constant voltage placed on the cavities caused the transit time effect to disappear. These experiments proved to be a good check on the previous conclusion that regardless of the amount of slip (within practical limits of beam stability), gain does not occur.

More through accident than for any other reason, it was discovered that gain could be obtained in this modified tube if the collector voltage were lowered to the range 50-150 volts. The output curves vs. drift tube voltage (See Figure 15) so nearly resembled those of Haeff that it was thought that the effect might be the same one. It was later learned that this could not have been the case, for Haeff's collector potential was much too high, as examination of his data showed. The effect was traced to secondary electrons at low velocity from the collector. These electrons were focussed back through the cavities and drift tube, reflected from the region in front of the cathode, and refocussed through the tube. These secondary electrons, having energy approximately equal to that of the primary beam less the collector potential, could not for

energy reasons return to the cathode. While this sort of multiple focusing might seem to be a matter of low probability, with carefully adjusted gun voltages and collector voltage, the primary and secondary beams interacted as a double stream to produce a gain of about 30 db greater than the magnitude of the space charge waves or fundamental mode. The net gain of the device was never positive, but since the space charge wave gain (klystron gain) of a tube may be made many db, the mechanism could produce net gain if used in a tube with more efficient and well-matched cavities.

Analysis was carried out to determine if the collector voltage, drift tube voltage, and beam current were consistent with double stream operation. Double stream theory gives as the condition for maximum gain the condition $\frac{\omega_o}{\omega} \frac{V}{\Delta V} = \text{a constant near unity}$. The ΔV here is approximately the collector voltage. The condition, written in terms of current and voltages, may be expressed at constant frequency as $IV_{DR, Tube}^{3/2} / V_{collector}^2 = \text{const}$. Data was taken by maximizing gain, and is presented in Figure 16. The curves, which should be a family of parabolas, are reasonable approximations thereto. For maximum gain, the constant $\frac{\omega_o V}{\omega \Delta V}$ can not be much less than unity. The values found experimentally are in quite good agreement with this. Anomalies in the data were due to multiple peaks in the gain maximum, which in turn were due to improper focussing at certain voltages. To obtain really maximized gain, it was necessary to use a magnetic collector assembly, carefully adjusted voltages, and a large magnetic field.

The large drift tube was replaced once more by the tapes, and measurements proved that while some double stream interaction was present at the same voltages as before, the smaller drift tube did not allow secondaries to return as readily and gain was reduced to the order of one or two db.

In the process of attempting to determine the origin of the gain, one idea which came forth was that electrons reflected elastically from the collector and at an angle to the axis were picked up by the magnetic

field and refocussed at lowered longitudinal velocity down the tube. Electrons which have transverse energy of 20 volts or more, at magnetic field strength of 500 gauss, describe transverse spiral motion in a radius of a small fraction of a millimeter. Such electrons would have little difficulty passing through the system, and would behave in much the same way as those observed. The expected number of elastically reflected electrons is only a few percent of the primary electrons, so there is a problem of magnitudes here. In tubes built by Haeff, grids at the gun end could produce secondaries and transversely focussed electrons which could explain the gains obtained. This is taken up in Appendix 4.

J. A. Reutz, of the RCA Laboratories, has made tests on a helix type traveling wave tube which show effect of low velocity secondaries from the collector. This is done by measuring the interaction of the beam with a helix wave traveling in the "backward" direction, from collector toward gun. For a particular tube with 130 microamperes primary beam current, the reverse current produced interaction equivalent to 8 microamperes current in the reverse direction; undoubtedly in the measurement on the demountable tube the secondary current was much higher. Ignorance of the surface condition of the collector, which is subject to contamination from several sources, makes it difficult to correlate the data with that of the two-cavity tubes.

SELECTED BIBLIOGRAPHY

1. Birdsall, C. K., *Interaction Between Two Electron Streams for Microwave Amplification*, Technical Report No. 36, Electronics Research Laboratory, Standord University, Palo Alto, California.
2. Haeff, A. V., *The Electron Wave Tube*, Proceedings of the Institute of Radio Engineers, 37, pp. 4-10, January, 1949.
3. Hahn, W. C., *Samll Signal Theory of Velocity-Modulated Electron Beams*, General Electric Review, June, 1939, pp. 258-270.
4. Haus, H., *A Multivelocitv-Electron-Stream In a Cylindrical Drift Tube*, unpublished report, Research Laboratory of Electronics, Massachusetts Institute of Technology, June 5, 1952.
5. Kemble, E. C., *The Fundamental Principles of Quantum Mechanics*, McGraw-Hill, 1937, pp. 90-112.
6. Macfarlane, G. G., and H. G. Hay, *Wave Propagation in a Slipping Stream of Electrons: Small Amplitude Theory*, Proceedings of the Physical Society, B, June, 1950, pp. 409-426.
7. Milne, W. E., *Numerical Calculus*, Princeton University Press, 1949, pp. 134-136.
8. Nergaard, L. S., *Analysis of a Simple Model of a Two-Beam Growing-Wave Tube*, RCA Review, IX, December, 1948, pp. 585-601.
9. Parzen, P., *Theory of Space Charge Waves in Cylindrical Waveguides With Many Beams*, Electrical Communication, September, 1951, pp. 217-219.
10. Pierce, J. R., and W. B. Hebenstreit, *A New Type of High-Frequency Amplifier*, Bell System Technical Journal, January, 1949, pp. 31-51.
11. Pierce, J. R., *Double-Stream Amplifier*, Proc. I.R.E., September, 1949, pp. 980-985.
12. Ramo, S., *The Electronic-Wave Theory of Velocity Modulation Tubes*, Proc. I.R.E., December, 1939, pp. 757-763.
13. Tien, P. K., L. M. Field, and D. A. Watkins, *Amplification by Acceleration and Deceleration of a Single-Velocity Stream*, Correspondence, Proc. I.R.E., February, 1951, p. 194.

APPENDIX 1

DERIVATION OF THE WAVE EQUATION. SIMPLE SOLUTIONS

The problem of wave propagation in an electron beam which has varying velocity across its cross section can be set up in general coordinates by use of Maxwell's equations.

$$\nabla \times \bar{\mathbf{H}} = \rho \bar{\mathbf{v}} + \epsilon_0 \frac{\partial \bar{\mathbf{E}}}{\partial t} \quad (\text{A1})$$

$$\nabla \times \bar{\mathbf{E}} = -\mu_0 \frac{\partial \bar{\mathbf{H}}}{\partial t} \quad (\text{A2})$$

$$\nabla \cdot \bar{\mathbf{E}} = \frac{\rho}{\epsilon_0} \quad (\text{A3})$$

$$\nabla \cdot \bar{\mathbf{H}} = 0 \quad (\text{A4})$$

plus the continuity equation

$$\nabla \cdot (\rho \bar{\mathbf{v}}) = -\frac{\partial \rho}{\partial t} \quad (\text{A5})$$

and the force equation

$$\frac{d}{dt} (m\bar{\mathbf{v}}) = -e(\bar{\mathbf{E}} + \bar{\mathbf{v}} \times \bar{\mathbf{B}}) \quad ; \quad \frac{d}{dt} = \frac{\partial}{\partial t} + \frac{\partial}{\partial x} \frac{\partial \mathbf{x}}{\partial t} + \frac{\partial}{\partial y} \frac{\partial \mathbf{y}}{\partial t} + \frac{\partial}{\partial z} \frac{\partial \mathbf{z}}{\partial t} \quad (\text{A6})$$

These equations are well known. The total derivative of $\bar{\mathbf{v}}$ in (A6) indicates the Lagrangian form of this equation, in which the observer moves with a particular electron.

The physical situation we wish to solve is described as follows: an electron beam is collimated so that it drifts in the z direction. An infinite (or nearly so) magnetic field prevents the electrons from having transverse velocity (directions perpendicular to the z axis will be called transverse). The electron beam must flow so that the disturbances in the beam caused by signal are single valued functions. This condition

is thought to be met in most small-signal tubes. Another condition to be required is that the disturbances are much smaller than the static values of space charge density ρ and velocity \bar{v} , so that products of disturbance terms are small compared to products of static and disturbance terms. Space charge density and velocity are assumed to be of the form $\rho_0 + \rho_1$ and $v_0 + v_1$, where subscript 1 indicates the AC or disturbance part, and 0 the static part.

It is assumed that if the excitation on the beam is sinusoidal, the output will be sinusoidal; all product terms of AC parts must be dropped. The type of solution assumed is a wave propagating as $e^{j\omega t - \gamma z}$. Derivatives with respect to z and t are respectively $-\gamma$ and $j\omega$.

If the curl of equation (A2) is taken and (A1) substituted, making use of the identity $\nabla \times \nabla \times \bar{A} = \nabla(\nabla \cdot \bar{A}) - \nabla^2 \bar{A}$, there obtains

$$\nabla(\nabla \cdot \bar{E}) - \nabla^2 \bar{E} = -\mu_0 \frac{\partial}{\partial t}(\rho \bar{v}) - \mu_0 \epsilon_0 \frac{\partial^2 \bar{E}}{\partial t^2} \quad (\text{A7})$$

The infinite collimating field requires all but the z component of \bar{v} to vanish, and eliminates the $\bar{v} \times \bar{B}$ term in (A6). The vector Laplacian can be broken up into z -directed and transverse components, $\bar{a}_z \nabla^2 \bar{E}_z + \nabla_t^2 \bar{E}_t$. It will be understood that $e^{j\omega t - \gamma z}$ is omitted from all quantities \bar{E} , ρ , \bar{v} in the equations, and will be understood to be a common factor of all. In Cartesian coordinates the transverse terms are vector components in transverse directions, and dependent on transverse electric field components. The mode of interest is what has been called the transverse magnetic (TM) mode in electromagnetic wave guiding structures. To obtain the propagation constant of this type of wave, the z component of (A7) alone is needed. This is

$$\frac{\partial}{\partial z} \left(\frac{\rho}{\epsilon} \right) - \nabla^2 \bar{E}_z = -\mu_0 \frac{\partial}{\partial t}(\rho v) - \mu_0 \epsilon_0 \frac{\partial^2 \bar{E}_z}{\partial t^2} \quad (\text{A8})$$

Using the linearizing approximations, (A5) becomes

$$\nabla \cdot (\rho_0 \bar{v}_1 + \rho_1 \bar{v}_0 + \rho_0 \bar{v}_0) = - \frac{\partial \rho_1}{\partial t} \quad .$$

The perturbed part is

$$\rho_0 \frac{\partial v_1}{\partial z} + v_0 \frac{\partial \rho_1}{\partial z} = -\frac{\partial \rho_1}{\partial t} ; -\gamma \rho_0 v_1 - \gamma v_0 \rho_1 = -j\omega \rho_1 \quad (\text{A9})$$

It can be reduced to give the relation between AC velocity and charge density.

$$\rho_1 = \frac{\gamma \rho_0}{j\omega - \gamma v_0} \cdot v_1 \quad (\text{A10})$$

Since the velocity is z-directed, (A6) becomes

$$\frac{\partial v_1}{\partial t} + \frac{\partial v_1}{\partial z} v_0 = -\frac{e}{m} E_z ; j\omega v_1 - \gamma v_0 v_1 = -\frac{e}{m} E_z . \quad (\text{A11})$$

It gives the relation between AC field and velocity. The two equations (A10) and (A11) may be combined to give the relation between charge density and field.

$$\rho_1 = -\frac{\gamma \rho_0 \frac{e}{m}}{(j\omega - \gamma v_0)^2} \cdot E_z \quad (\text{A12})$$

Now, we have (A8), which tells the field which will be produced by a certain charge density and velocity. (A11) and (A12) tell the charge density and velocity set up by a given electric field. The combination may be used to eliminate ρ_1 and v_1 . There results the equation

$$-\nabla^2 E_z - \frac{\omega^2}{c^2} E_z + \frac{\gamma^2 \rho_0 \frac{e}{m}}{(j\omega - \gamma v_0)^2} E_z + \frac{\omega^2}{c^2} \frac{\rho_0 \frac{e}{m} \epsilon}{(j\omega - \gamma v_0)^2} E_z = 0 . \quad (\text{A13})$$

The Laplacian ∇^2 may be broken up into z and transverse components. The z component is a second derivative with respect to z and the transverse part depends on the coordinate system. For Cartesian coordinates,

$$\nabla^2 \phi = \frac{\partial^2 \phi}{\partial x^2} + \frac{\partial^2 \phi}{\partial y^2} + \frac{\partial^2 \phi}{\partial z^2} , \text{ and for cylindrical coordinates}$$

$$\nabla^2 \phi = \frac{1}{r} \frac{\partial}{\partial r} \left(r \frac{\partial \phi}{\partial r} \right) + \frac{1}{r^2} \frac{\partial^2 \phi}{\partial \theta^2} + \frac{\partial^2 \phi}{\partial z^2} . \text{ The final wave equation, in these two}$$

coordinate systems, is

$$\frac{\partial^2 E_z}{\partial x^2} + \frac{\partial^2 E_z}{\partial y^2} + \left(\gamma^2 + \frac{\omega^2}{c^2} \right) \left(1 + \frac{\omega_0^2}{(j\omega - \gamma v_0)^2} \right) E_z = 0 \quad (\text{A14})$$

$$\frac{1}{r} \frac{\partial}{\partial r} \left(r \frac{\partial E_z}{\partial r} \right) + \frac{1}{r^2} \frac{\partial^2 E_z}{\partial \theta^2} + \left(\gamma^2 + \frac{\omega^2}{c^2} \right) \left(1 + \frac{\omega_o^2}{(j\omega - \gamma v_o)^2} \right) E_z = 0 \quad (\text{A15})$$

Here $-\rho_o \frac{e}{m\epsilon}$ has been replaced by ω_o^2 , the square of the plasma angular frequency.

For tubes with circular cylindrical beams and no variation of excitation in the θ direction, the θ derivative disappears. In Cartesian systems in which the beam is infinite in the y direction, the y derivative disappears. These two cases are the ones discussed in the text.

There is nothing in the above derivation which prohibits the use of more than one velocity group of electrons in the beam at the same position. If this is the case, the $\frac{\omega_o^2}{(j\omega - \gamma v_o)^2}$ term is replaced by a sum of such terms, for the total space charge density is a sum of the partial ones, and the AC electric field is common to all.

Simple solutions. About the simplest type of solution which can be imagined is one obtained by making E_z independent of transverse coordinates. The propagation equation reduces to the criterion $1 + \frac{\omega_o^2}{(j\omega - \gamma v_o)^2} = 0$. v_o must of course be independent of coordinates. The resulting values of γ are $j \frac{(\omega \pm \omega_o)}{v_o}$. The two values indicate two waves, one traveling faster, the other slower than the electrons. Only when there is coupling and the waves grow is it possible to isolate these two waves. The solutions are thus of the form $e^{j(\omega t - \frac{\omega}{v_o} z \pm \frac{\omega_o}{v_o} z)}$, and may be combined as $e^{(\omega t - \frac{\omega}{v_o} z)} \frac{\sin(\frac{\omega_o}{v_o} z)}{\cos(\frac{\omega_o}{v_o} z)}$. All quantities vary in this fashion, so that if at one point along the beam the AC charge density was zero, it would have successive zeros at positions corresponding to $\Delta z = \frac{\pi v_o}{\omega_o}$. This is approximately the case in a non-infinite beam, for the solutions for γ can be written $j \frac{(\omega \pm p\omega_o)}{v_o}$, in which p is a reduction factor less than unity. In finite beams, the term $1 + \frac{\omega_o^2}{(j\omega - \gamma v_o)^2}$ must be some negative quantity, in order that the solution for E_z decay outside the beam limits, and the result is a smaller effective ω_o . Physically, this effective reduction of ω_o can be explained by the diverging of the electric flux lines. The smaller the diameter of the beam compared to the distance between bunches, the more R.F.

electric field is external to the beam, and less internal.

When the beam is a mixture of electrons of different velocities, but is still of infinite cross-section, the simple criterion becomes

$$1 + \sum_n \frac{\omega_{on}^2}{(j\omega - \gamma v_{on})^2} = 0. \quad \text{This is taken up in Appendix 2.}$$

The significance of the term "plasma frequency" which is applied to ω_o may be appreciated if the conditions in a beam not in uniform motion are studied. Let us assume a collection of electrons infinite in the x, y plane electron group is excited by a field in the z direction at frequency ω . The equations are now:

$$\frac{\partial E_z}{\partial z} = \frac{\rho_1}{\epsilon_o} ; \quad \rho_o \frac{\partial v}{\partial z} = -\frac{\partial \rho_1}{\partial t} ; \quad \frac{e}{m_1} E_z = \frac{\partial v_1}{\partial t}$$

They have the solution $\omega = \omega_o$. This indicates that an electron plasma will, if disturbed, oscillate at undiminishing amplitude at the frequency ω_o ; this is one way of explaining what happens in a modulated beam. The minima observed are points where the oscillation is instantaneously zero.

APPENDIX 2

MIXED BEAMS

A problem very similar to that of the slipping stream is that of the modes of propagation of a mixture of electrons of different velocity, such that in every part of the cross section the distribution of velocities among the electrons is the same. The general criterion for this, set up by Haeff, is obtainable from the equations of Appendix 1 and is

$$\int_0^{\infty} \frac{f'(v_0) dv_0}{(j\omega - \gamma v_0)^2} = -1, \quad (\text{A16})$$

where $f'(v_0)$ is defined by $\frac{e}{m\epsilon} d\rho = f'(v_0) dv_0$, and is the distribution function of velocity. If only discrete velocities are present, the integral becomes a sum. The problem of two discrete velocity classes was discussed by Haeff in a manner which left in question the results of adding a third class. In order to illustrate the general problem of a continuous velocity distribution, the writer has used several graphical representations. In the first of these, we plot the locus of the function $\frac{1}{(j\omega - \gamma v_0)^2}$ for a particular argument of γ . In Figure 17 are shown steps in the development of this locus, which is cardioidal. A value of $\text{Arg } \gamma$ which is in the gain region has been chosen. The satisfaction of the criterion is brought about by adding vectors drawn from the origin to the locus; the length of each vector is weighted by the ω_0^2 for the group of electrons at that velocity. Two vectors are indicated which can be summed to equal -1. The weighting factor of each vector depends on the charge at the particular velocity it represents. The regions A, A' of the figure are regions where a small amount of charge will help the most in the summation. The region B is one where charge contributions will deteriorate the sum. It stands to reason that charge velocities in the B region cannot help to produce gain, and need to be offset by even greater charge in the A and A' regions. The B region, referring back to the locus

of $j\omega - \gamma v$, corresponds to electron velocities and wave velocity almost equal. It follows from this that the addition of a beam of intermediate velocity to a set of two beams will always deteriorate the gain. This method of presentation does not indicate how much the gain is deteriorated, but only shows how much more charge must be added to return it to status quo.

A presentation which does indicate the effect of the addition of other beams may be set up. Consider the left hand side of (A16), in its summation form, $\sum_n \frac{\omega_{on}^2}{(j\omega - \gamma v_n)^2}$, as a function in the complex γ plane. This function is completely defined if the charge density of each velocity class is given. The function has double poles at $\gamma = j\frac{\omega}{v_n}$, corresponding to each beam velocity whose magnitudes are proportional to the charge density at each velocity. The characteristic values of γ are defined as the -1's of the function. It is observed that for imaginary γ the function is always negative. A plot showing lines of constant magnitude and phase of this function for a system of two velocity classes is shown in Figure 17. If the magnitudes of the poles are small, all -1's fall on the imaginary γ axis (no gain). If the poles are large, and equal, the -1's fall on their perpendicular bisector. If they are unequal, the -1's fall nearer the lesser pole. Figure 18 also shows the results of adding a third velocity class of intermediate velocity. The result is much the same as for each of the two outer pairs of poles singly. The gain modes of a group of velocity classes in a mixed beam are similar to those due to the interaction between adjacent velocity classes. This is believed to be an important result, a fundamental reason why there is no amplification in a slipping stream.

Finite mixed beams. Birdsall (1) and Haus (4) analyzed the effect of finite size of a mixed beam, and the effect of continuous velocity classes. The conclusions are much the same as above. The method of analysis of a finite Cartesian or cylindrical beam is relatively simple, since the form of the equations (A14) and (A15) and zero boundary conditions calls for $1 - \int_0^\infty \frac{f'(v_o) dv_o}{(j\omega - \gamma v_o)^2} = k^2$ and k^2 may be obtained from function

tables. In the Cartesian case, $k^2 = \left(\frac{n\pi}{a}\right)^2$, where a is the beam width, and n is an integer. The resulting solutions are infinite in number, but because detecting systems can only detect readily the first mode ($n = 1$) this is the only solution of practical interest.

The solutions of Haus in a continuous velocity distribution involve taking a partial integral, which reduces the order of the singularity at $j\frac{\omega}{v_0}$ to unity. This can be represented by an analogue consisting of a two-dimensional electric charge distribution, whose distribution function is the derivative of the velocity distribution function $f'(v_0)$ of the original problem.

APPENDIX 3

VELOCITY DISTRIBUTIONS

Cylindrical beam. A cylindrical beam in a infinitely strong magnetic field will travel in a straight line, and the electron velocity at any point in its cross section will have a velocity dependent on the electric potential there. Because of the negative sign of the space charge, the potential at the center of the beam will be reduced over that at the edge.

Consider a beam of circular cross section, traveling down a circular tube of equal or greater diameter and of infinite length. The space charge density is assumed uniform over the entire cross section. Under these conditions, Poisson's law (equation (A3)) becomes

$$\begin{aligned}\frac{1}{r} \frac{d}{dr} \left(r \frac{dV}{dr} \right) &= -\frac{\rho}{\epsilon_0} ; \quad -\frac{dV}{dr} \doteq E_r \\ r \frac{dV}{dr} &= -\frac{\rho r^2}{2\epsilon_0} + c_1 \\ \frac{dV}{dr} &= -\frac{\rho r}{2\epsilon_0} + \frac{c_1}{r} \\ V &= -\frac{\rho r^2}{4\epsilon_0} + c_1 \ln r + c_2\end{aligned}\tag{A17}$$

c_1 and c_2 are constants of integration.

Since no line charge exists at the origin, the solution within the beam has $c_1 = 0$. Outside the beam, ρ is zero, and c_1 is required to make the solution match at the boundary. Within the beam, the voltage may be expressed as

$$V = V_0 - \frac{\rho r^2}{4\epsilon_0} .\tag{A18}$$

If the velocity corresponding to this potential is calculated,

$$v_o^2 = \frac{2e}{m} V_o - \frac{\rho e}{2m\epsilon_o} r^2 = \frac{2e}{m} V_o + \frac{\omega_o^2 r^2}{2} = v_{o0}^2 \left(1 + \frac{\omega_o^2 r^2}{2v_{o0}^2}\right),$$

and, making the assumption that the velocity difference is small compared to the absolute velocity, there is obtained

$$v_o \simeq v_{o0} + \frac{\omega_o^2 r^2}{4v_{o0}}. \quad (\text{A19})$$

v_{o0} is the velocity at the center of the beam and ω_o the usual plasma (angular) frequency. This is the velocity distribution which was used in the computational code.

If the beam does not completely fill the tube in which it is enclosed, there results a voltage at the beam center which is even less than that when the beam fills the tube. This means that there must be a longitudinal field at the point where the beam enters this tube. If the tube is too large, the beam may be unstable by virtue of the large potential difference. Therefore, it pays to make the tube as small as possible in practical experiments when it is desired to obtain the highest beam currents.

Cartesian beam. The type of beam discussed here is one which extends to infinity in the y direction, but is of finite width in the x direction. It travels in the z direction, as usual, and so the Poisson equation is simply

$$\frac{d^2V}{dx^2} = -\frac{\rho}{\epsilon_o}$$

$$V = -\frac{\rho x^2}{2\epsilon_o} + c_1 x + c_2 \quad (\text{A20})$$

The beam here may be enclosed by conductors of any potential at both sides of the beam. Both the linear and the squared term in the voltage may be present. If c_1 and c_2 are made such values that the voltage across the beam is a perfect square of a linear function of x, the velocity will be linear in x. The voltage will then vary as $(x - a)^2$, and the velocity as $(x - a)$. All that is necessary to produce this condition is

to apply correct voltages to the side plates.

In the parabolic voltage distribution,

$$V = \frac{\rho(x-a)^2}{2\epsilon_0} = \frac{1}{2} \frac{m}{e} v_0^2$$

$$v_0 = \omega_0(x-a) ; \frac{dv_0}{dx} = \omega_0 \quad (\text{A21})$$

The velocity gradient is seen to be exactly equal to ω_0 , a result which is highly useful.

APPENDIX 4

ANALYSIS OF HAEFF'S DATA

Through the generosity of the Naval Research Laboratory, the author obtained permission to review the data taken on the single stream amplifying tubes. The tubes were built and operated by Mr. R. S. Ware, who was working with Dr. Haeff at that time, but has since left the Laboratory. At the time this review was made, the work described in this dissertation was 95% complete.

The main object was to determine whether the gain found by Haeff could have been due to the same phenomenon as discovered by us, that of secondary electrons forming a double stream. The possibility of these being collector secondaries was quickly discounted when it was discovered that throughout the work at NRL, the collectors were maintained at a voltage 300v. greater than that of the output cavity, which was in turn always about 450v. or more above the cathode potential.

The types of tubes used by Haeff had nothing out of the ordinary in their construction through the cavities and drift region. The cavities had been removed from 707 type klystron tubes, and the drift tube was a $\frac{1}{2}$ inch diameter by 12 inch long non-magnetic tube. The collector was of tantalum, formed into a long cone into which the electrons penetrated.

The first single stream tube was actually a double stream amplifier with only a single cathode operative. The cathode was a directly heated, thoria coated tungsten zig-zag of maximum dimensions around $\frac{1}{2}$ inch. This was followed by a grid, maintained at positive voltage, with wires perpendicular to those of the cathode. This tube gave many decibels of gain, more gain at times than when used as a double stream amplifier. The data shows that it was necessary to carefully adjust the grid voltage, the magnetic field, and even the cathode current(!). Grid voltage for

best gain was near 40 volts, which leads us to believe that it was secondaries from the grid which caused double stream interaction. In this tube the intercepted current on this and a following grid was as high as 53 out of 60 milliamperes, with an additional 3 ma. caught by the cavity grids. The number of secondary electrons released under these conditions would certainly be of the same order of magnitude as the primary current.

Another tube on which data was taken and amplification discovered had an accelerating grid with somewhat higher voltage. Another tube had a grid with voltages as high as 500. This latter tube could not possibly be explained on the basis of secondary electrons, for none of the electrodes had appropriate voltages. It is necessary to devise some new explanation, and the following is thought to be a credible one.

All electrons in an electron beam formed by a gridless (or gridded) gun designed for parallel electron flow and confined by a very high magnetic field have essentially the same longitudinal velocity. As the magnetic field is weakened, the electron paths can no longer be straight if transverse velocities have been introduced by the gun structure. The electrons will follow a spiral path, and the longitudinal component of velocity will be smaller than before. In a gun with very close cathode-grid spacing (positive grid) many of the electrons have appreciable transverse velocity especially if, as in the tube used by Haeff, the gun is temperature limited. The electrons with transverse velocities should have continuously distributed longitudinal velocities, but if the magnetic field is low, the spiral paths of some of the electrons may carry them into the side of an aperture plate, rather than through the aperture. Those of a group of electrons of greater transverse velocity may come to a focus on the aperture and pass through to the drift region, thus forming, along with the straight-line-path electrons a double stream of two different ranges of longitudinal velocity. It will be remarked that the limiting aperture of the gun used was much smaller than the cavity and drift tube diameter. The above described phenomenon may occur as shown in Figure 18.

The question has been raised as to whether the source of Haeff's gain might have been the velocity jump occurring between the cavities and the drift tube. This may be disposed of by calculating the gain, which for voltage ratios of 3 to 1 would be about 7 db. Since all observed gains were much higher, even at voltage ratios less than this, it is impossible to account for the gain in this way. Dr. Rudolph Kompfner, now of Bell Telephone Laboratories, has communicated to the writer that, following receipt of a NRL report, he built a single stream tube and obtained large gains, but maximum gain was obtained at the lowest drift tube voltage manageable, 25 volts, with a voltage ratio of 80.

The Haeff data is further questionable in that, in much of the experimentation, difficulty was encountered with ion or electron oscillations in the gun. This might have caused some trouble, since it was not indicated whether the output signal with zero input was indeed zero. At another point in the data, a graph showed gain vs. system pressure. This curve showed pressures definitely in the range where ions could change focussing. The gain decreased greatly as pressure went up, probably indicating that the sensitive focussing conditions were destroyed in the presence of ions.

The source of the gain in Haeff's tubes may yet be questioned, but we believe that only the source of the second (low-velocity) part of the beam is in question. The facts have been given as fairly and objectively as possible; since the tubes reported on no longer exist, it would be difficult to find out more about them. In the light of our experience, we feel that it is not necessary longer to assume the gain a mystery.

APPENDIX 5

WAVES IN TWO LINEARLY COUPLED SYSTEMS WITH DIFFERENT PHASE VELOCITIES

Here it will be illustrated that the coupled waves formed when two waves of different phase velocity interact linearly can grow with distance. This growing wave must have phase velocity intermediate to those of the original sources.

Let us consider two uncoupled waves traveling with different velocity and in the same direction. Let us consider two planes A and B perpendicular to the wave motion such that the two waves, assumed to be harmonic functions (scalar or vector) progress θ_1 and θ_2 in phase, respectively, between the two planes; in other words the distance A-B is $\frac{\theta_1}{2\pi}$ wavelengths for wave 1 and $\frac{\theta_2}{2\pi}$ wavelength for wave 2.

A form of linear coupling which is suitably general is a discrete coupling constant k and discrete distance between points of coupling. If with zero coupling, the 1st wave is described by a quantity E_1 at A and $E_1 e^{j\theta_1}$ at B, then likewise E_2 , $E_2 e^{j\theta_2}$ describes the 2nd wave at A and B. With coupling, the first wave is E_1 at A and $[E_1 + kE_2] e^{j\theta_1}$ at B, likewise, with coupling, the second wave becomes E_2 , $[E_2 + kE_1] e^{j\theta_2}$. The coupling coefficient is assumed symmetrical for simplicity, but this is not necessary to prove existence of a growing wave. It stands to reason that bilateral coupling is necessary to a certain extent, for if one wave could perturb the other without the reverse, the second wave would just become like the first.

If the wave described by the coupled relations $[E_1 + kE_2] e^{j\theta_1}$ and $[E_2 + kE_1] e^{j\theta_2}$ at B is a true coupled wave, the ratio of the wave function at B to that at A must be the same for both sources.

$$\frac{E_1 + kE_2}{E_1} e^{j\theta_1} = \frac{E_2 + kE_1}{E_2} e^{j\theta_2} \quad (\text{A22})$$

This relation can be solved for $\frac{E_1}{E_2}$. Two values are found, given below

$$\frac{E_1}{E_2} = \frac{e^{j(\theta_1 - \theta_2)} - 1}{2k} \pm \sqrt{\frac{[e^{j(\theta_1 - \theta_2)} - 1]^2}{4k^2} + e^{j(\theta_1 - \theta_2)}} \quad (\text{A23})$$

Now, the ratio given, using $e^{j\theta} \approx 1 + j\theta$, for small θ_1 is

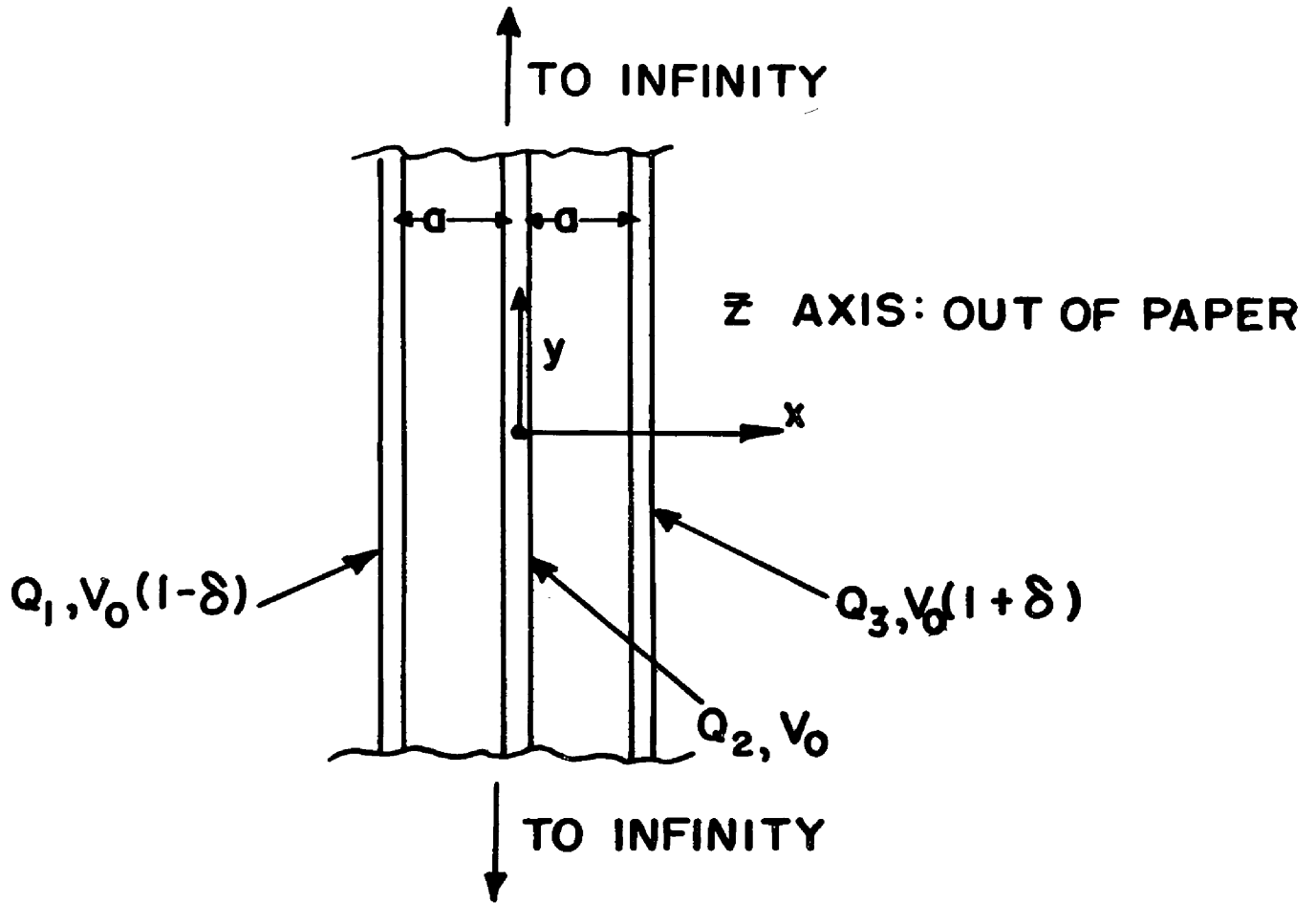
$$\frac{E_2 + kE_1}{E_2} e^{j\theta_2} \approx \left(1 + j \frac{[\theta_1 - \theta_2]}{2} \pm j \sqrt{\frac{(\theta_1 - \theta_2)^2 - k^2}{4}}\right) (1 + j\theta_2) \quad (\text{A24})$$

If this be simplified and the term $-\frac{\theta_2(\theta_1 - \theta_2)}{2}$ neglected, it becomes

$$1 + j \frac{\theta_1 + \theta_2}{2} \pm \sqrt{k^2 - \frac{(\theta_1 - \theta_2)^2}{4}} \quad (\text{A25})$$

Let us observe that the first two terms are the limit as $\theta_1, \theta_2 \rightarrow 0$, of $e^{j \frac{(\theta_1 - \theta_2)}{2}}$. The phase velocity of the coupled wave is intermediate to those of the uncoupled waves if $\sqrt{k^2 - \frac{(\theta_1 - \theta_2)^2}{4}}$ is real, for which the condition is $k > \frac{(\theta_1 - \theta_2)}{2}$. The term under the radical is the source of gain and attenuation waves, both of which are produced for sufficiently large k .

The above does not perfectly represent any actual amplifier where k may be a function of $\theta_1 - \theta_2$. A helix-type traveling wave tube has maximum gain, under certain conditions, when the beam and helix wave travel at the same speed, as given in (A25). The coupling of two beams in a double stream amplifier is non-amplifying when the difference in velocities is zero, but gain vanishes for sufficiently high difference. The most important feature of the analysis is the fact that phase velocity of the growing wave is between those of the original waves.



MODEL FOR 3-BEAM ANALYSIS

Figure 1. Cross section of model for analysis of three thin beams side by side.

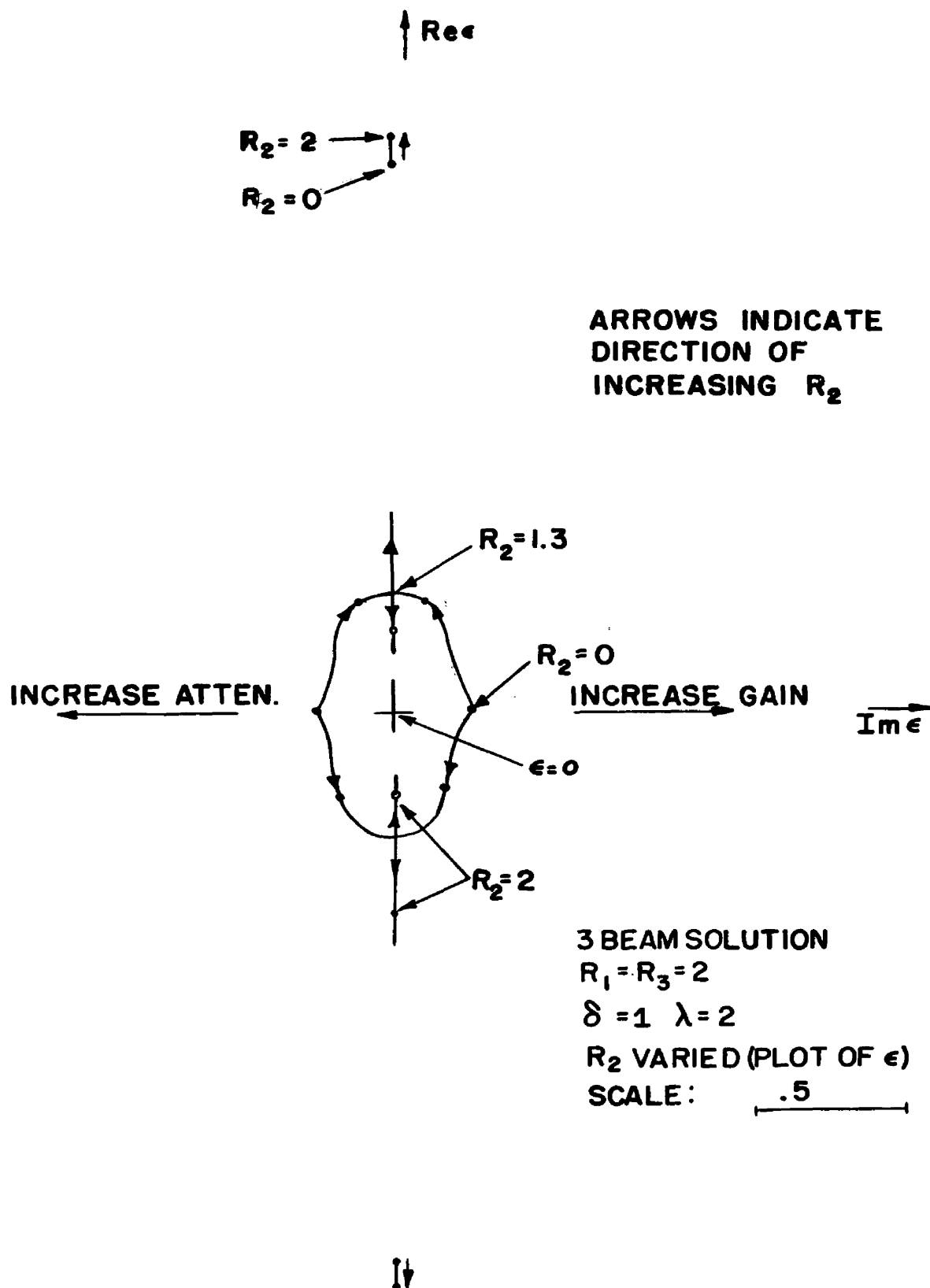


Figure 2. Loci of propagation constant versus current in center beam.

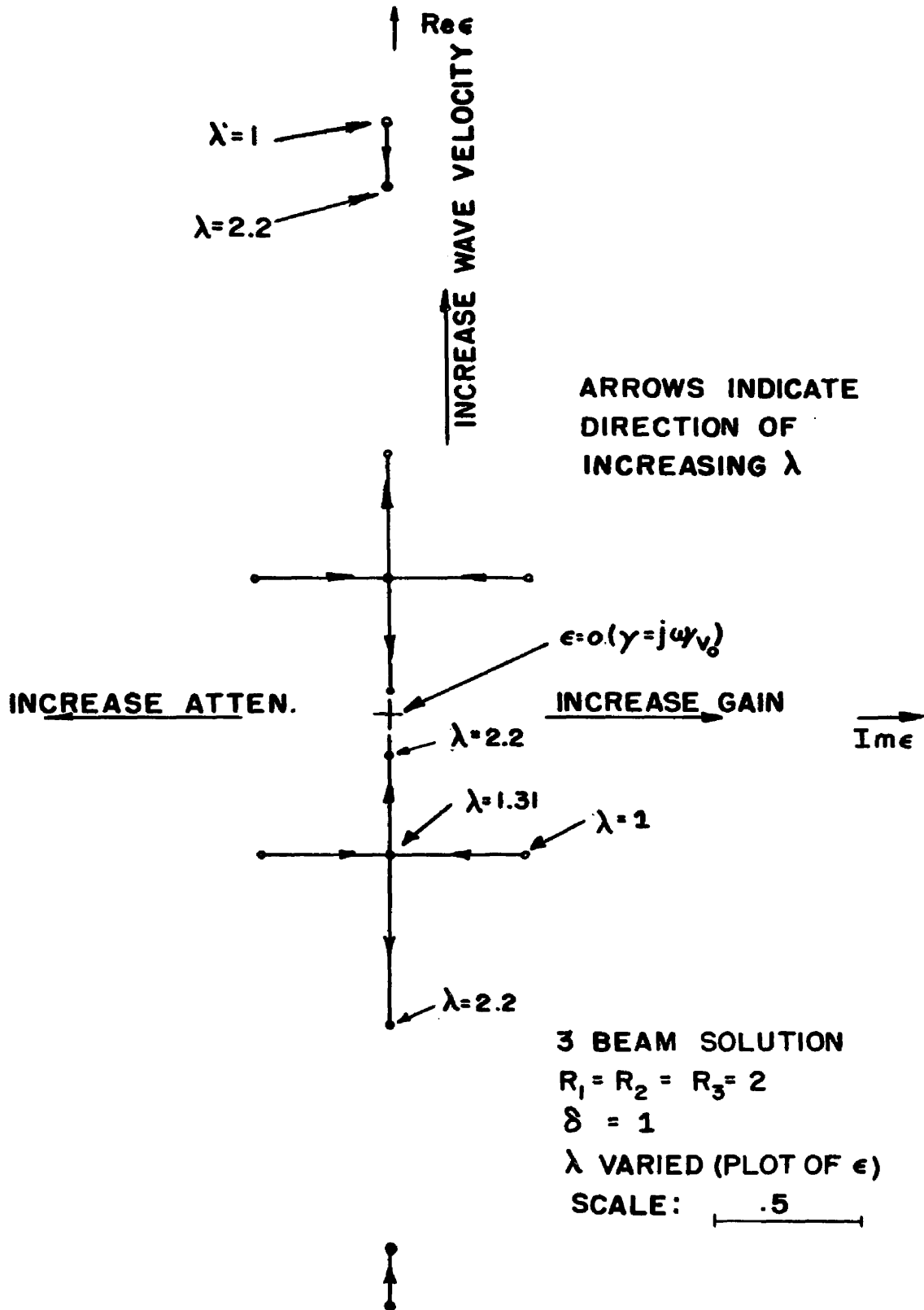


Figure 3.: Loci of propagation constant versus beam spacing parameter.

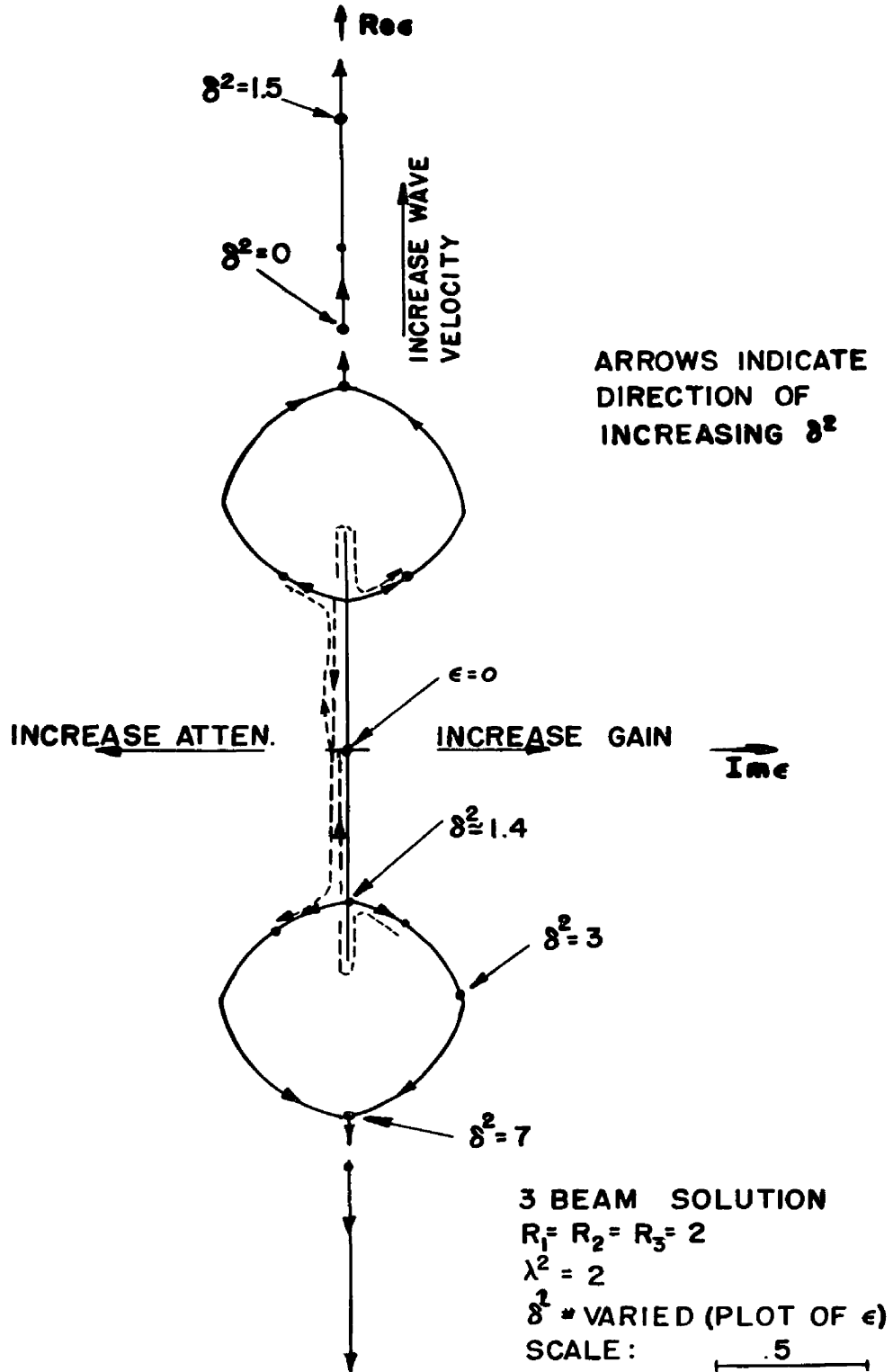
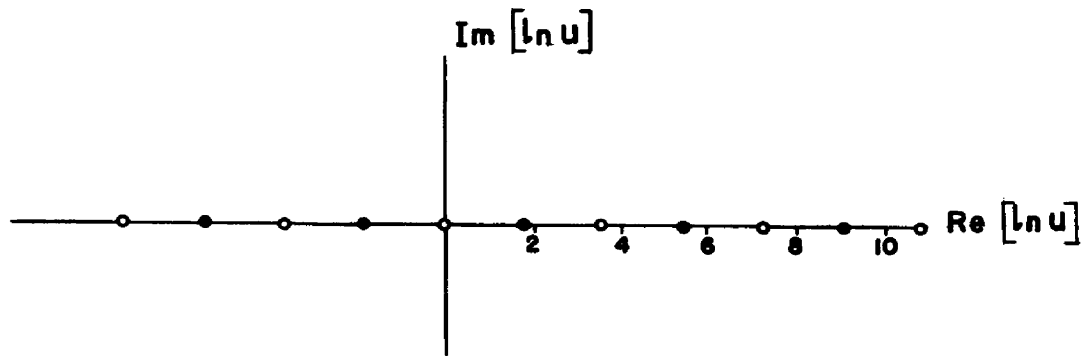


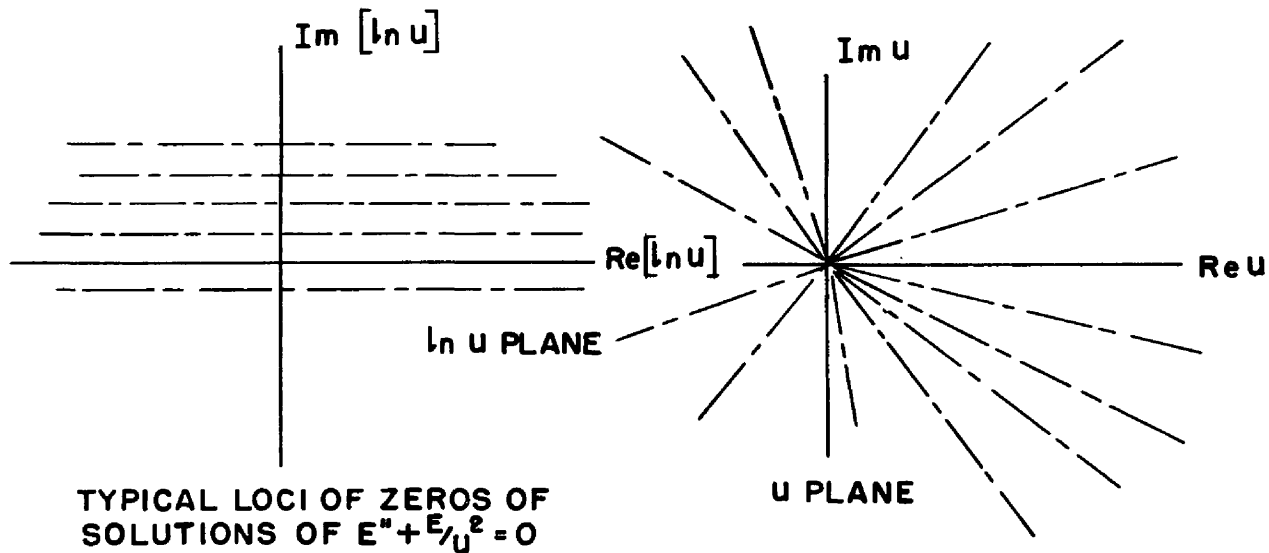
Figure 4. Loci of propagation constant versus fractional velocity separation.



ZEROS OF $\sqrt{u} \sin(.866 \ln u)$ AND $\sqrt{u} \cos(.866 \ln u)$
IN THE $\ln u$ PLANE

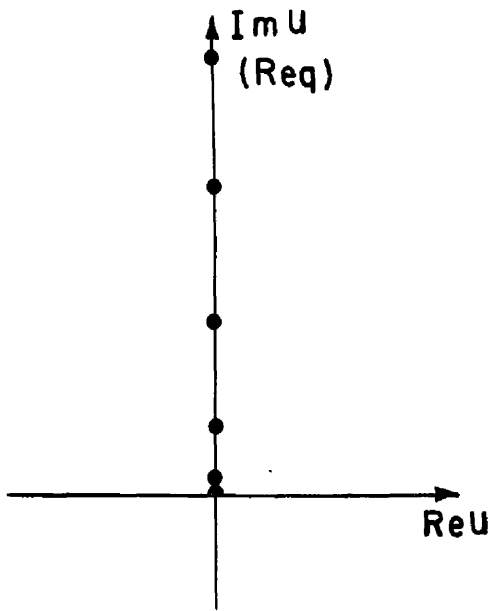
LEGEND:

- — ZERO OF SIN
- — ZERO OF COS

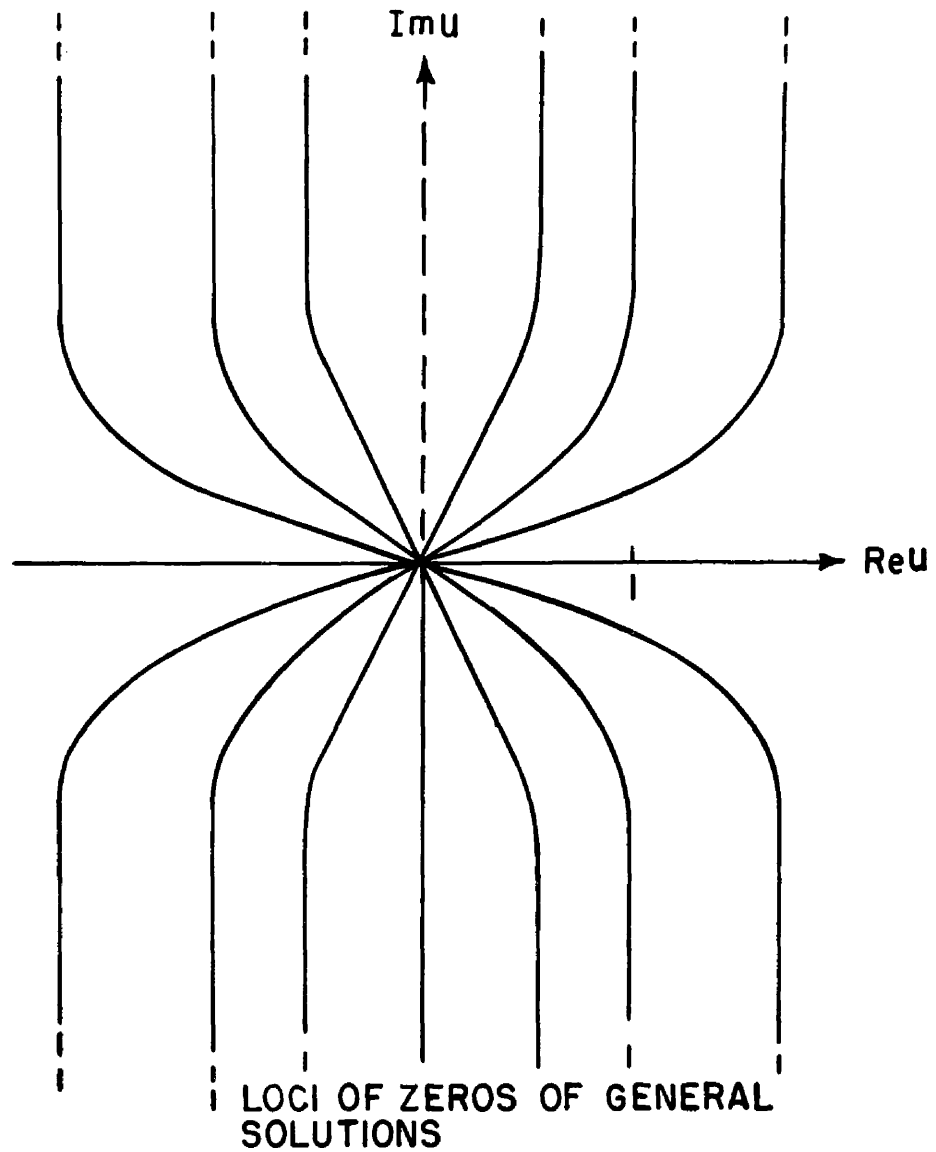


TYPICAL LOCI OF ZEROS OF SOLUTIONS OF $E'' + E/u^2 = 0$

Figure 5. Loci of zeros of solutions of Equation (11).



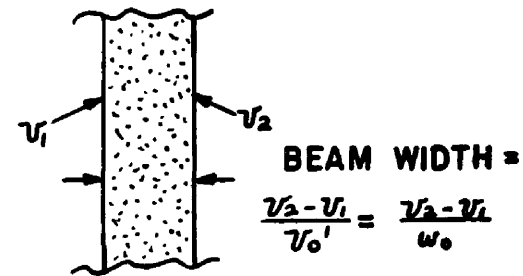
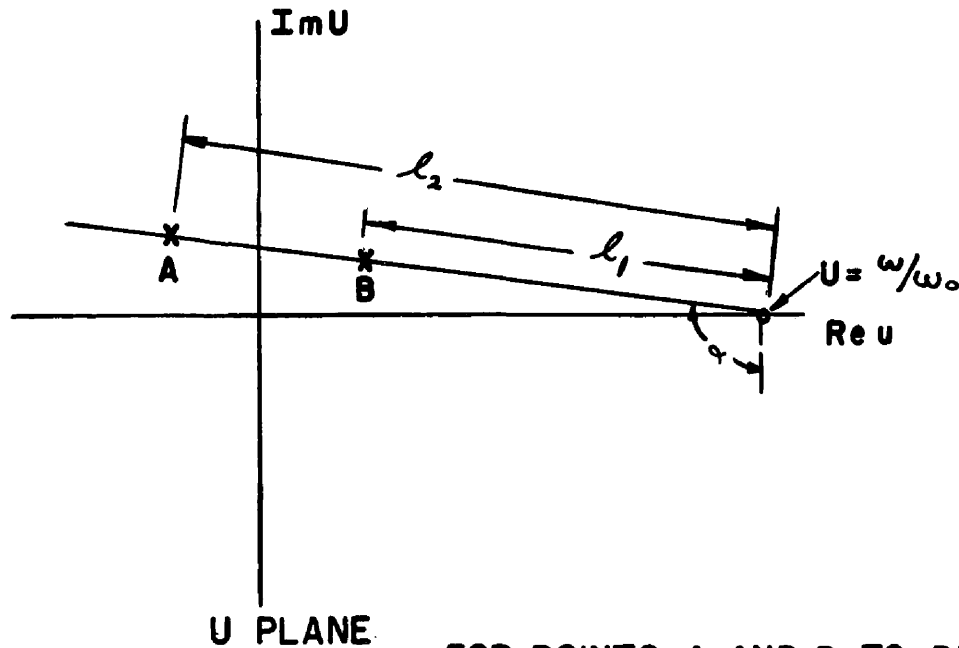
LOCUS OF ZEROS OF A PARTICULAR SOLUTION OF $\frac{d^2 E_z}{dq^2} + (1 + \frac{1}{q^2}) E_z = 0$ where $q = ju$



LOCI OF ZEROS OF GENERAL SOLUTIONS

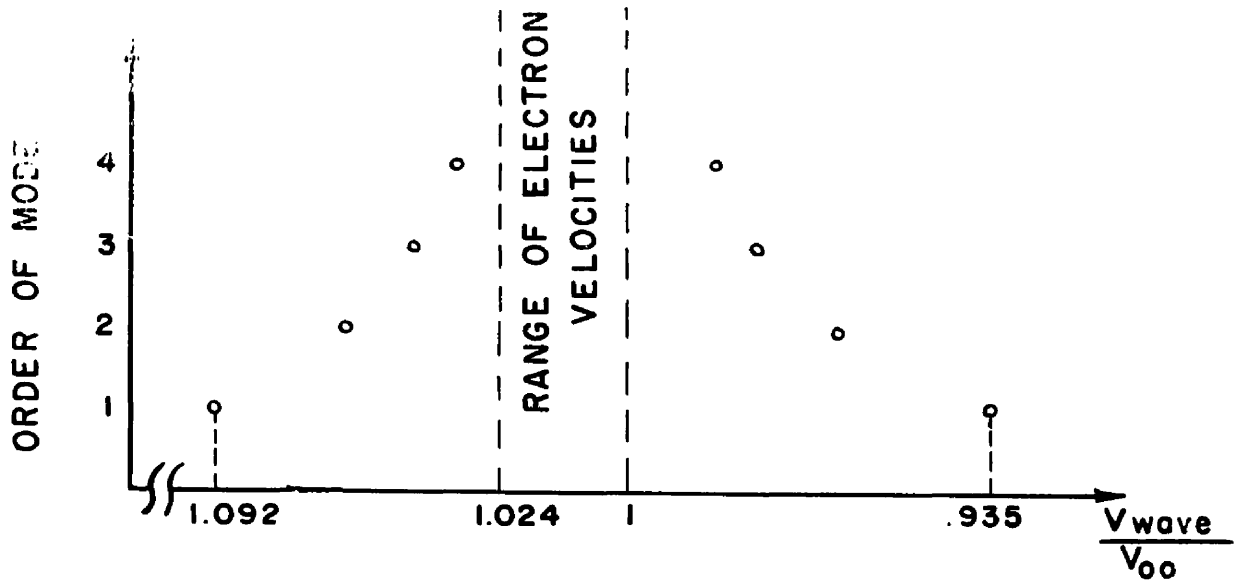
Figure 6. Loci of zeros of solutions of Equation (12)

CONDITIONS REQUIRED FOR SOLUTION,
IN THE U PLANE



FOR POINTS A AND B TO DEFINE A SOLUTION,
 $l_1/l_2 = v_1/v_2$, WHERE v_1, v_2 ARE VELOCITIES
AT THE BEAM EDGES. A LINE THRU A AND B
MUST INTERSECT THE RE U AXIS AT ω/ω_0
A AND B MUST BE ZEROS OF A SOLUTION
OF $E'' - (1 - \frac{1}{\mu^2}) E = 0$
 $|\gamma| = |l_1/v_1| = |l_2/v_2|$; $Arg \gamma = \alpha$

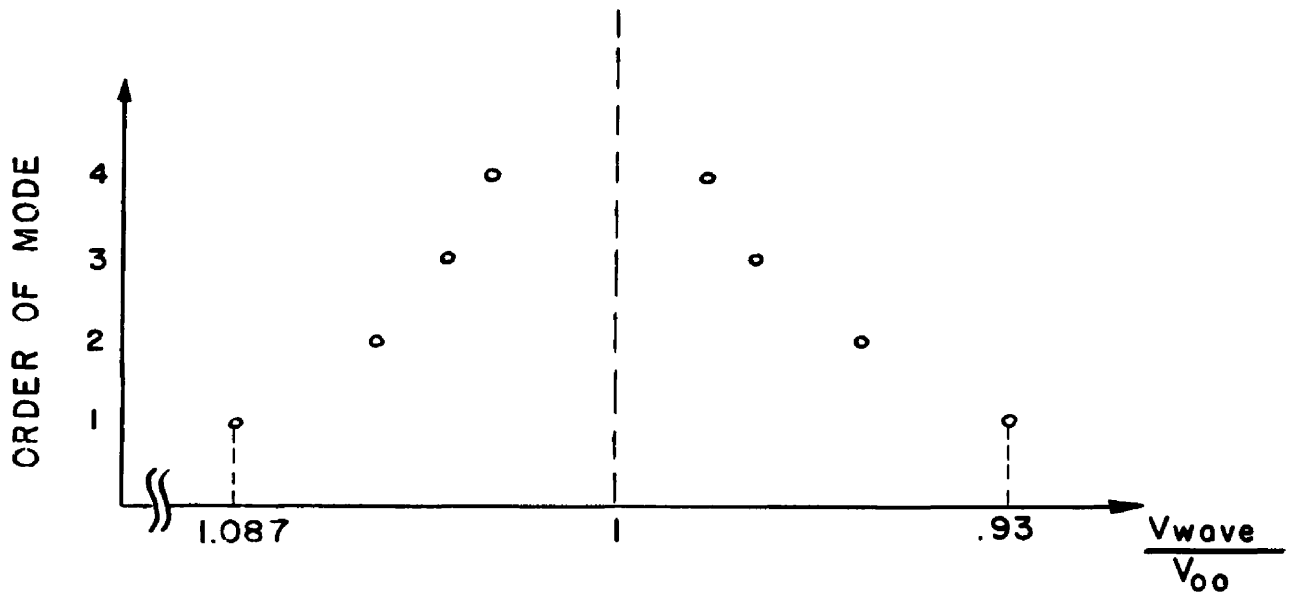
Figure 7. Geometric relations which must be satisfied at end points of solutions, Cartesian beam solution.



(A) BEAM WITH APPROXIMATELY 2.4 % SLIP

$\frac{\omega}{\omega_0} = 10$; $V_0 = 100^v$; BEAM RADIUS = 1mm.;

$f = 3000$ mc.; $I \approx 6$ ma.; BEAM FILLS DRIFT TUBE



(B) BEAM WITH UNIFORM VELOCITY V_{00}
SAME CONSTANTS

Figure 8. Computed velocities of fundamental and higher order modes of slipping and univelocity beams, cylindrical beam solution.

TWO CAVITY TUBE
(NOT TO SCALE)

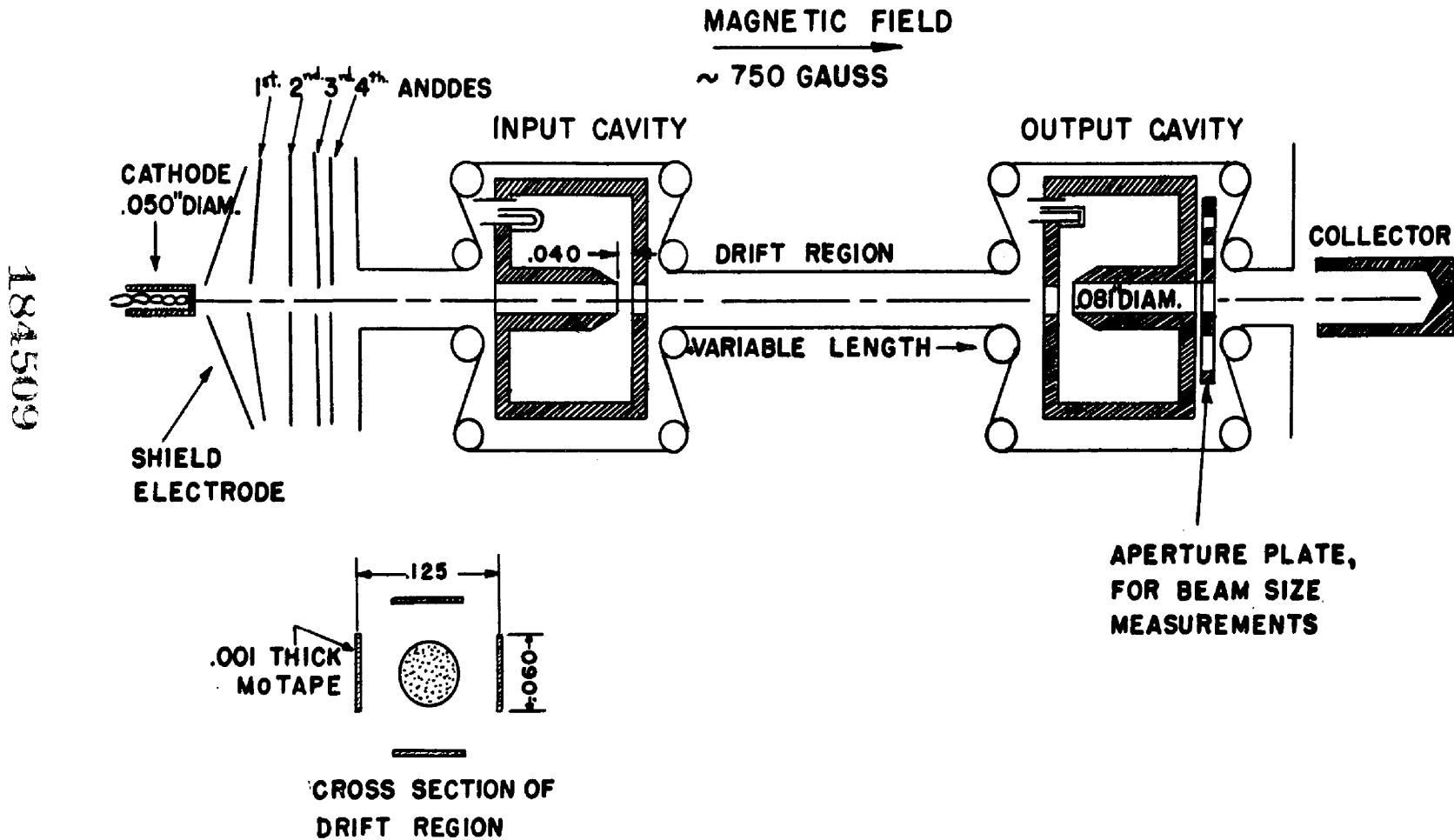


Figure 9. Diagram showing basic features of variable length two-cavity demountable tube.

RF MEASURING SYSTEM

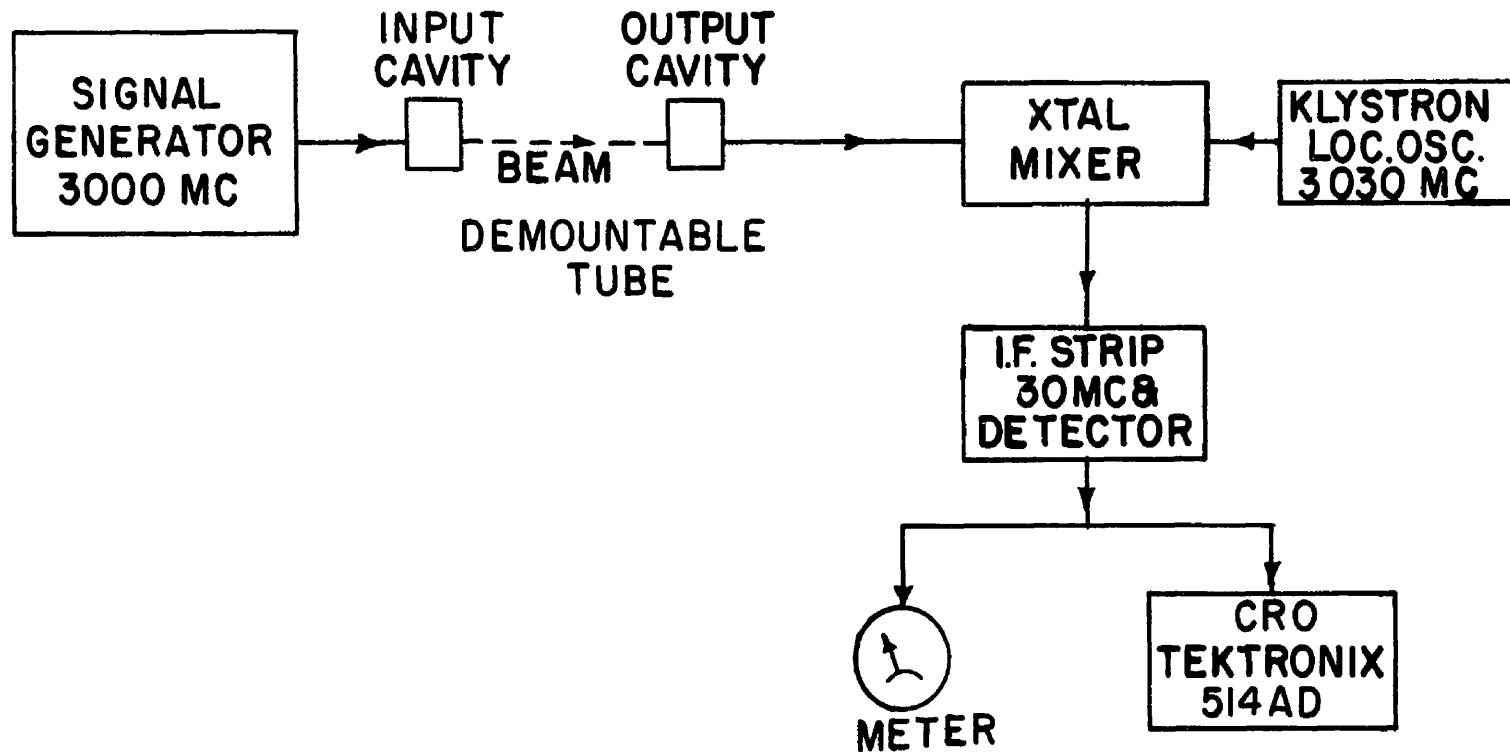
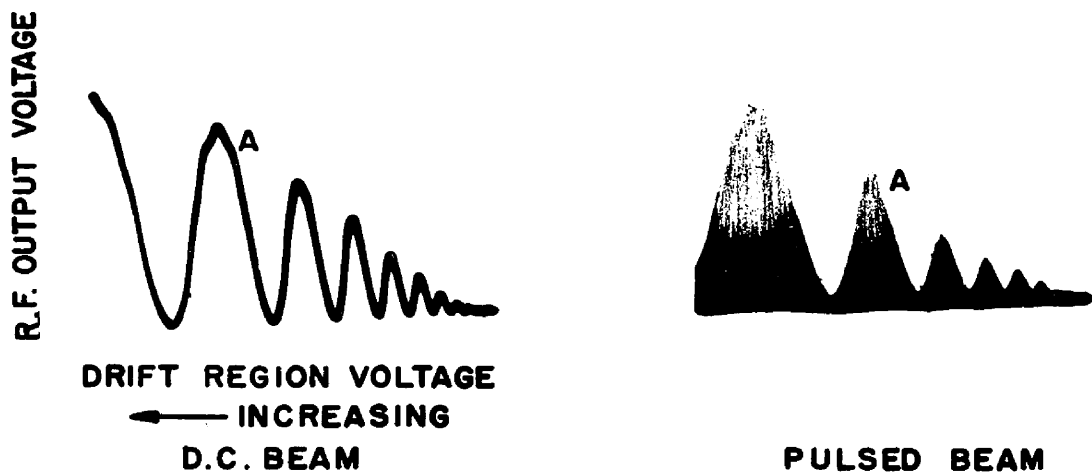


Figure 10. Block diagram of system used in experimental work.

COMPARISON OF SPACE CHARGE WAVES IN PULSED AND DC BEAMS. PULSE LENGTH 1μ SECOND; 5000 CYCLE RATE; CAVITY SPACING $11 \frac{3}{4}$ INCHES



BEAM CURRENT .8 MA

SLIGHTLY DIFFERENT VOLTAGE RANGES ARE USED FOR THE TWO TRACES ABOVE. CORRESPONDING PEAKS ARE MARKED "A"



BEAM CURRENT .68 MA

Figure 11. Output voltage vs. drift tube voltage, for pulsed and continuous single beam.

CAVITY OUTPUT vs. DRIFT REGION VOLTAGE
FOR 3 DIFFERENT DRIFT LENGTHS. BEAM
CURRENT .8 MA., FIXED R.F. INPUT

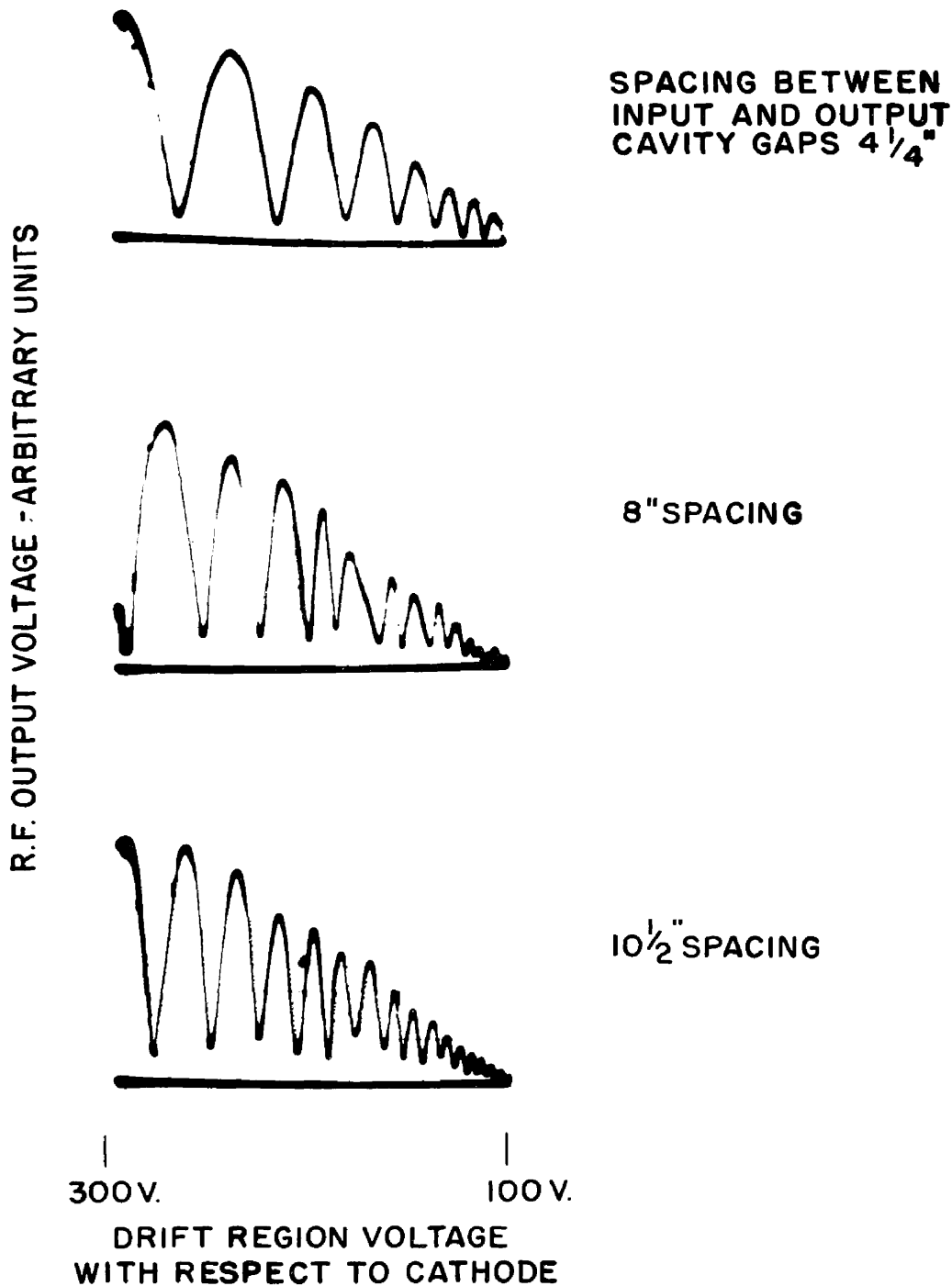


Figure 12. Observed output versus drift voltage for different drift lengths in two cavity demountable tube.

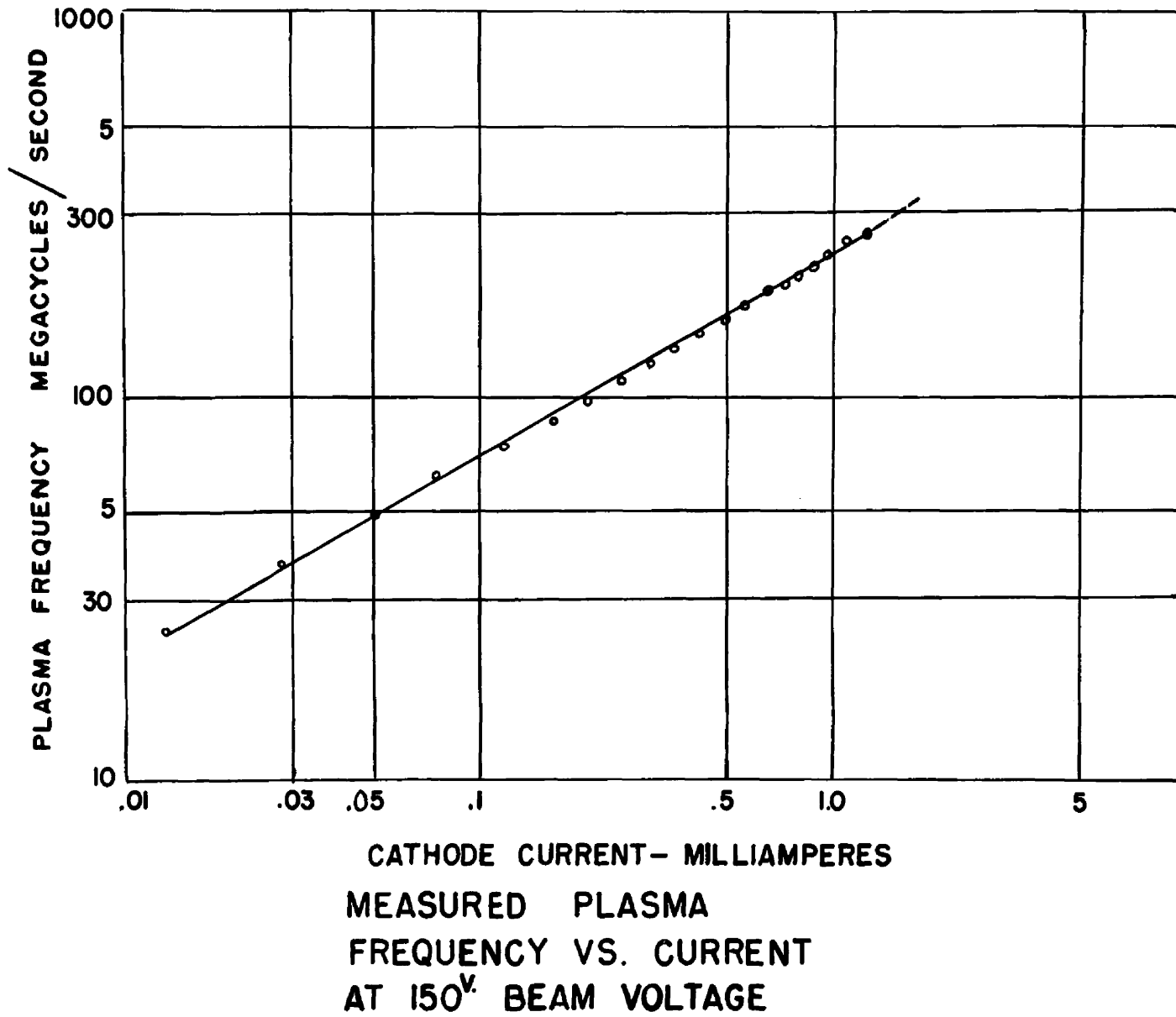


Figure 13. Electron plasma frequency from plasma wavelength measurements.

**TWO CAVITY TUBE WITH VARIABLE POTENTIAL
LARGE DIAMETER DRIFT REGION**

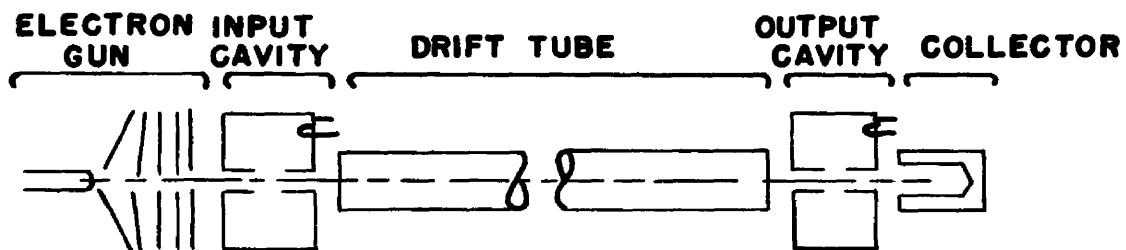
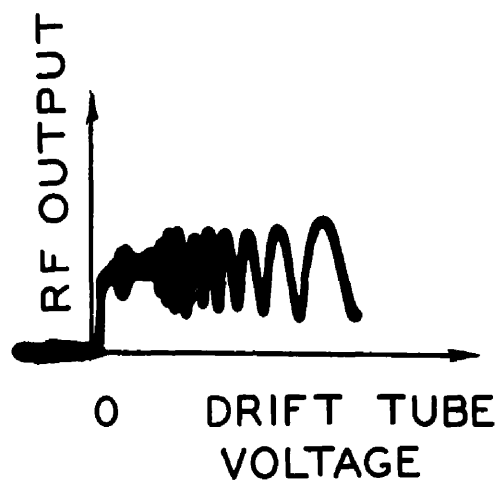


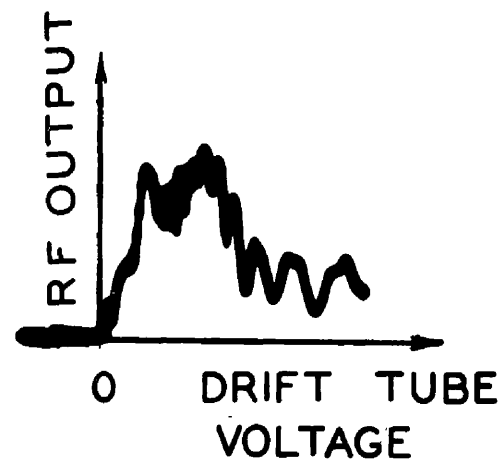
Figure 14. Basic parts of tube of the type used by Haeff.

GAIN OBSERVED AT LOW COLLECTOR VOLTAGE DUE TO DOUBLE STREAM EFFECT OF SECONDARY ELECTRONS.



(A) NORMAL COLLECTOR VOLTAGE

500 VOLTS



(B) LOWERED COLLECTOR VOLTAGE

70 VOLTS

CAVITY VOLTAGE 460^v.
BEAM CURRENT 3.3^{ma}.

Figure 15. Observed output voltages illustrating gain at low collector voltage.

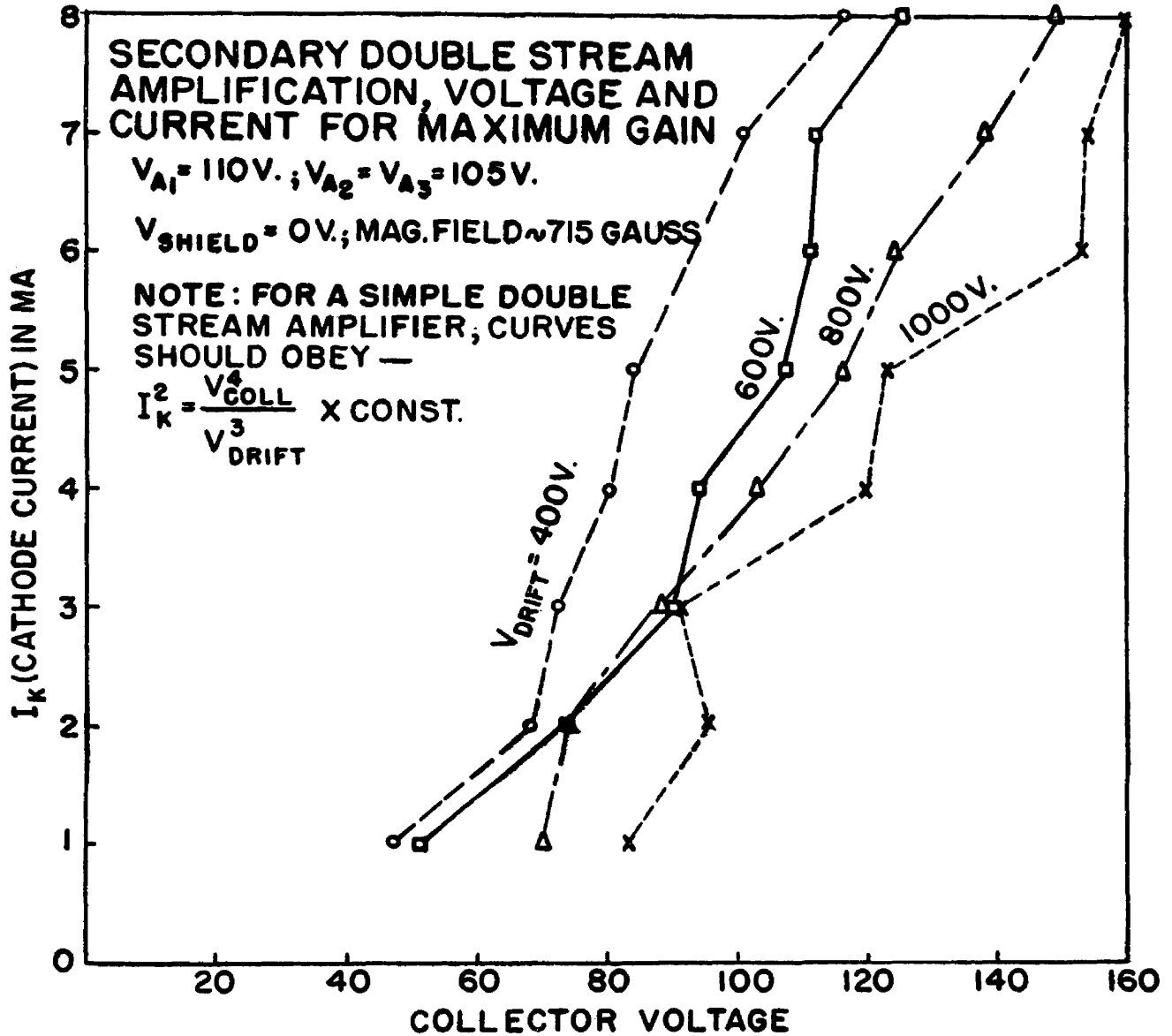
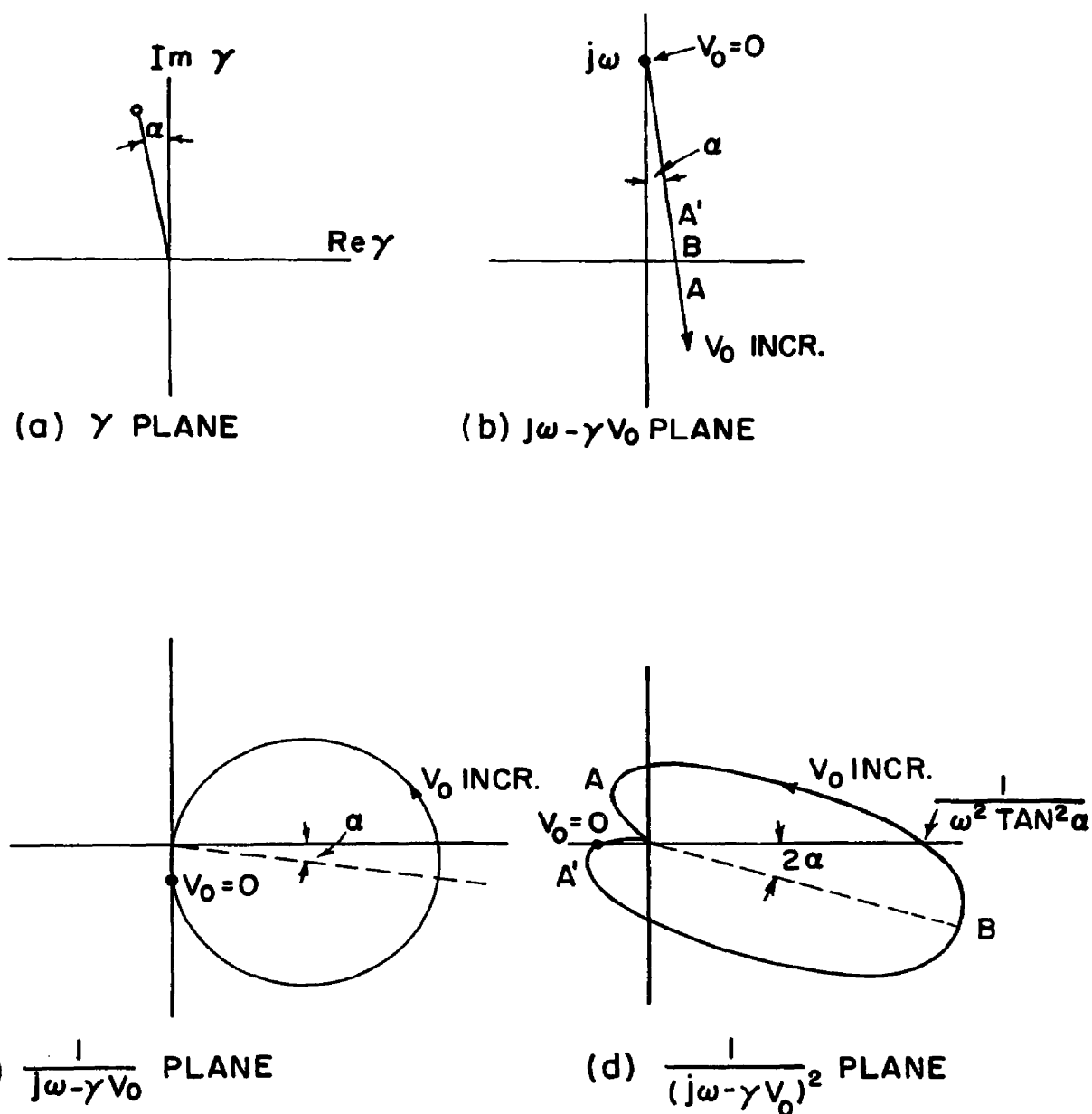
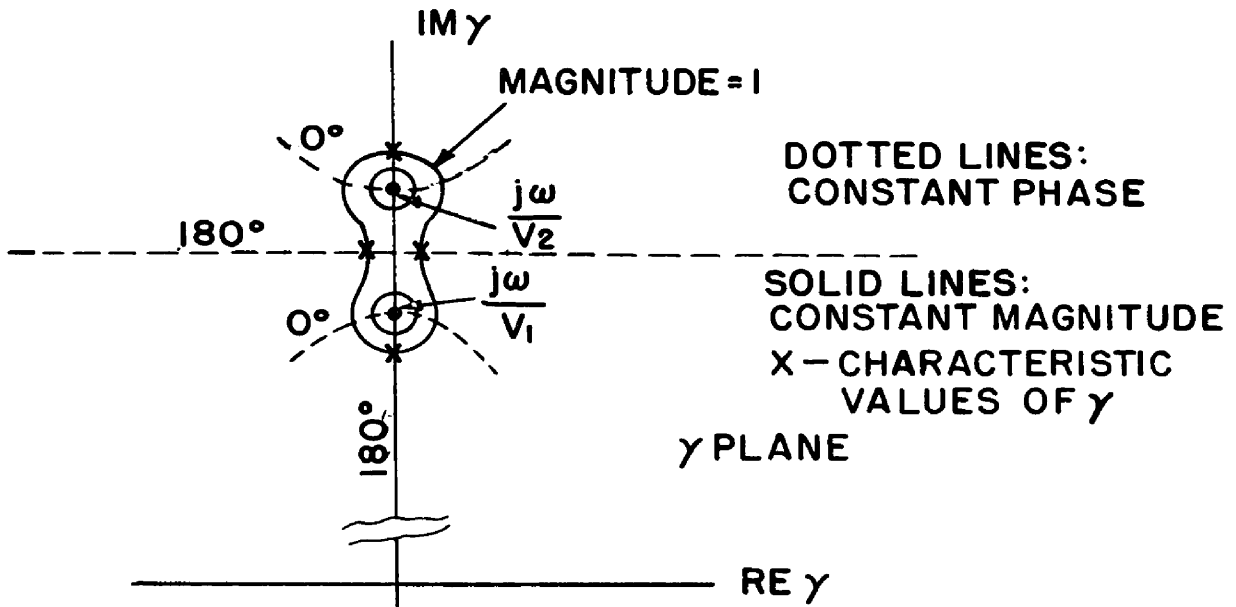


Figure 16. Experimental data showing similarity of output of tube with low collector voltage to that of a simple double stream amplifier. Theoretically, curves should be parabolic.

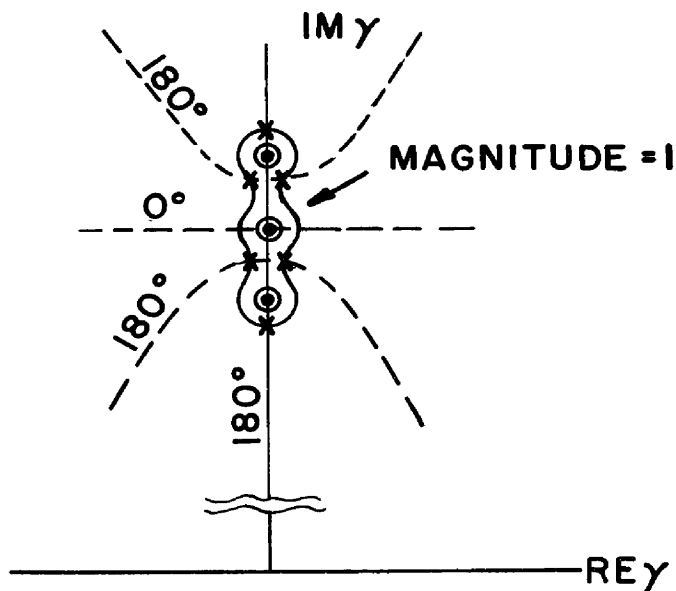


LOCUS OF $\frac{1}{(j\omega - \gamma V_0)^2}$ AS V_0 IS VARIED, FOR CHOSEN ARGUMENT OF $\gamma = (\frac{\pi}{2} + \alpha)$

Figure 17. Curves illustrating conditions for gain in a mixed beam.

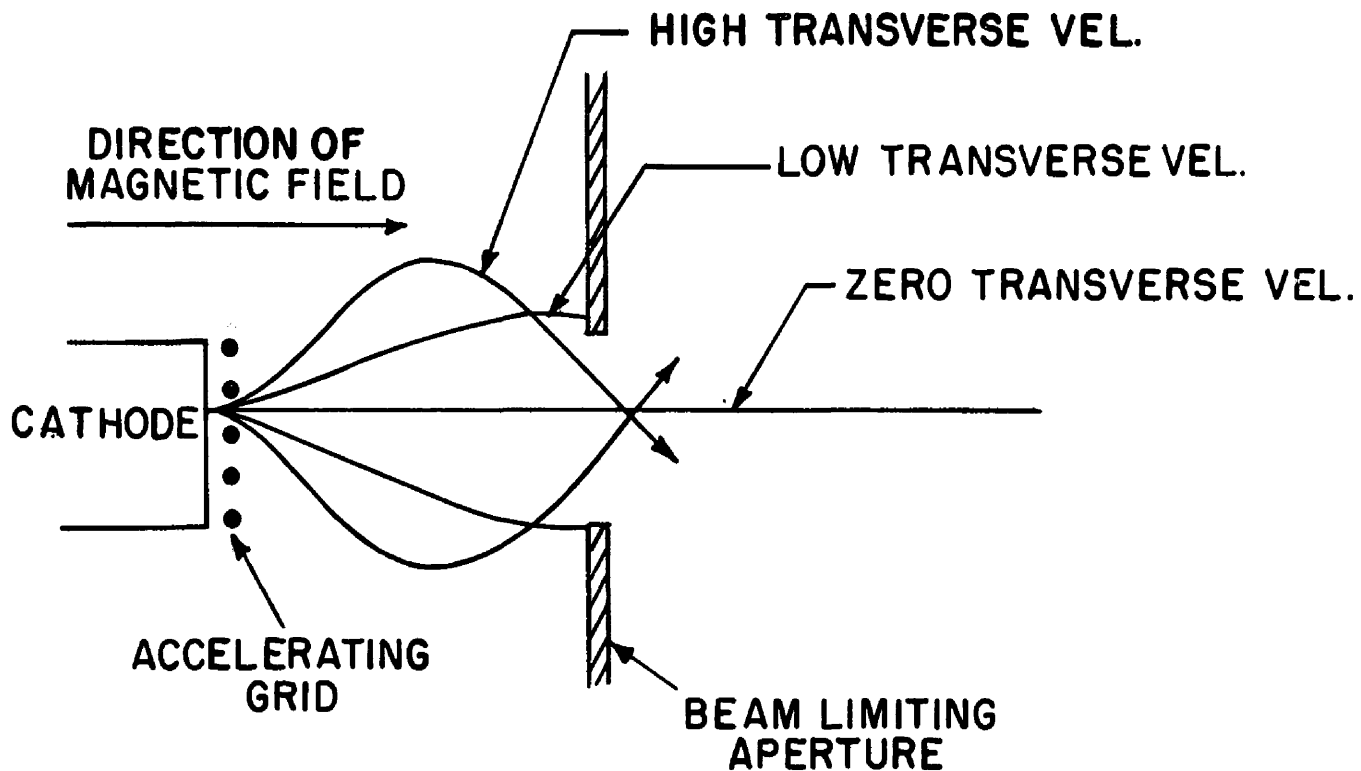


CONTOUR MAP OF $\sum_n \frac{\omega_{0n}}{(j\omega - \gamma v_n)^2}$ FOR A SYSTEM
OF TWO MIXED BEAMS



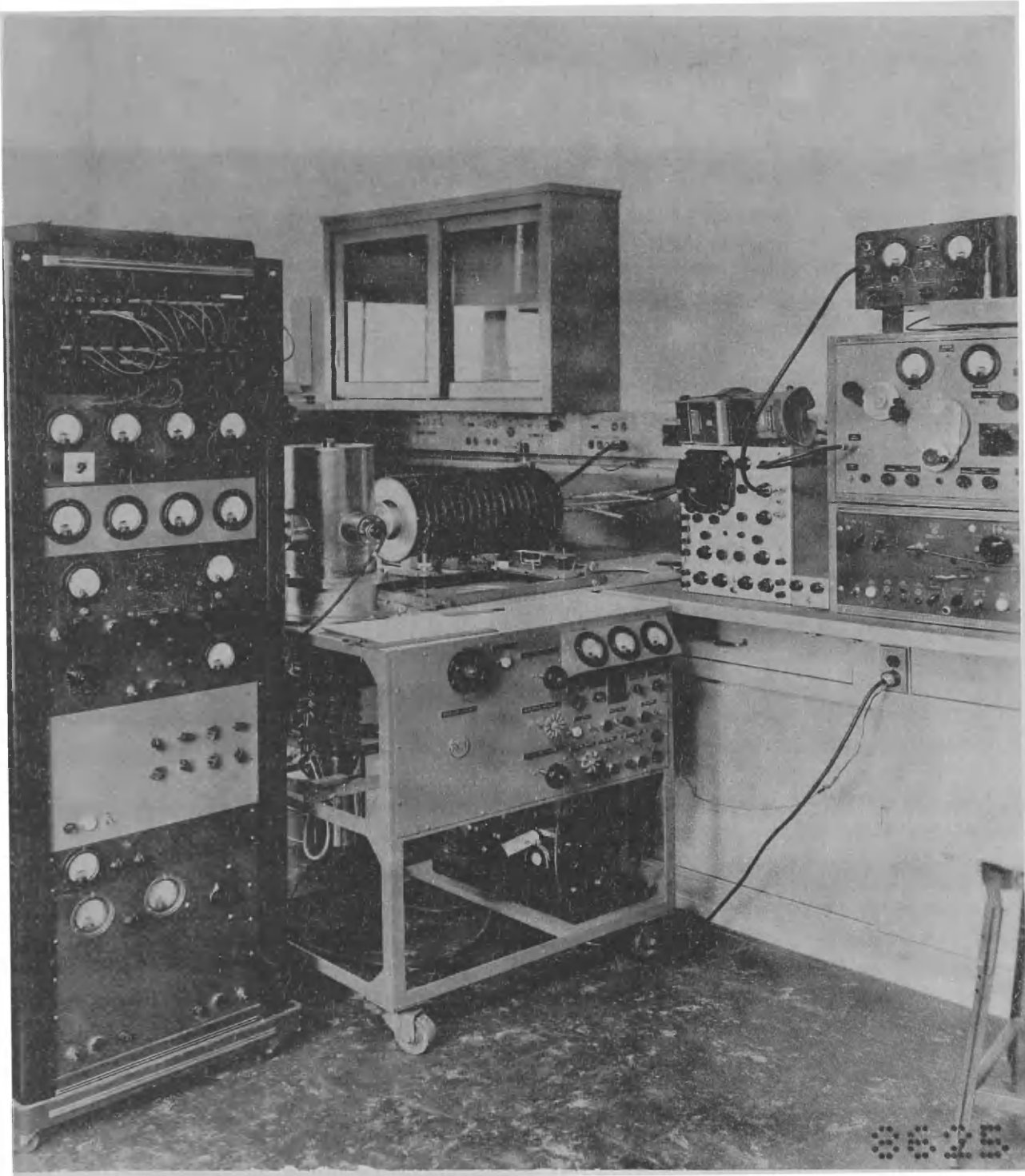
CONTOUR MAP FOR THREE MIXED BEAMS

Figure 18. Contour maps showing the effect of adding a third stream to a double stream amplifier.



SELECTIVE INTERCEPTION OF ELECTRONS WITH DISTRIBUTED TRANSVERSE VELOCITY

Figure 19. Hypothetical electron paths which would produce a double stream effect in a gridded gun.



COMPLETE TEST SETUP

Plate 1. Photograph of complete apparatus. Power supplies in rack at left, vacuum system in center, and RF equipment on bench at right.

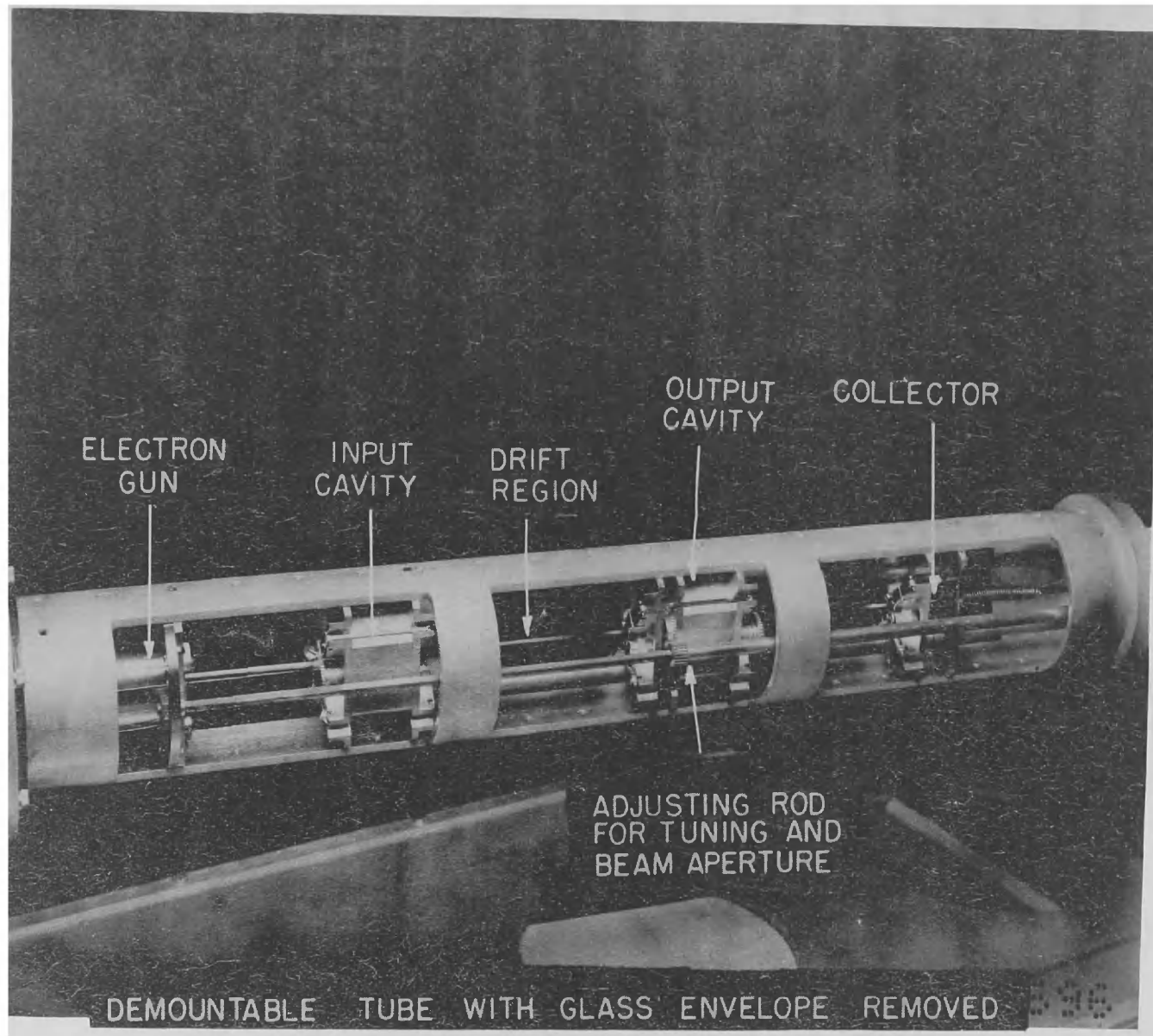


Plate 2. Closeup of demountable tube, illustrating construction and basic parts.

ACKNOWLEDGEMENTS

The author is deeply indebted to his advisor, Dr. Weber, for help and encouragement, particularly in the initial stages of this work; to the RCA Laboratories Division, which offered the opportunity to complete the problem, and especially to the Traveling Wave Tube group; and to Dr. Hermann Goldstine and Mr. Daniel Slotnick of the Institute for Advanced Study, whose cooperation enabled the computational work on cylindrical beams to be performed. The assistance received through them was in part made possible by a U. S. Army Ordnance Corps Contract.

We also wish to express appreciation for the fine job of typing done by Mrs. Jayne Toussaint, who was somehow able to decode the many additions and corrections in the manuscript.

Lastly, we wish to pay tribute to Dr. Andrei Haeff, without whose initial investigation and curiosity the problem discussed herein would not have existed.

VITA

Name: Walter Raleigh Bean

Permanent address: 9 Maguire Road, Hamilton Square, New Jersey

Degree: Doctor of Philosophy, 1953

Date of birth: August 27, 1928

Place of birth: Richmond, Virginia

Secondary education: E.C. Glass High School, Lynchburg, Virginia

Collegiate institutions attended	Dates	Degree	Date of Degree
University of Maryland	1943-	B.S.	June, 1947
	1953	M.S.	June, 1950
Catholic University	1950-52		

Employed 1947-1952 as Instructor in Electrical Engineering, University of Maryland. Engineer at Washington Institute of Technology, Inc. part time, 1947-49. Research engineer at R.C.A. Laboratories, Princeton, New Jersey, 1952 to present.